2016

DIFFUSE CO2 DEGASSING AND THE ORIGIN OF VOLCANIC GAS VARIABILITY FROM RINCÓN DE LA VIEJA, MIRAVALLES AND TENORIO VOLCANOES, GUANACASTE PROVINCE, COSTA RICA

Aurelia Liegler
aliegler@mtu.edu

DIFFUSE CO_2 DEGASSING AND THE ORIGIN OF VOLCANIC GAS VARIABILITY FROM RINCÓN DE LA VIEJA, MIRAVALLES AND TENORIO VOLCANOES, GUANACASTE PROVINCE, COSTA RICA

By

Aurelia Liegler

A THESIS

Submitted in partial fulfillment of the requirements for the degree of

MASTER OF SCIENCE

In Geology

MICHIGAN TECHNOLOGICAL UNIVERSITY

2016

This thesis has been approved in partial fulfillment of the requirements for the Degree of MASTER OF SCIENCE in Geology.

Department of Geological and Mining Engineering and Sciences

Thesis Advisor: *Chad D. Deering*

Committee Member: *Severine Moune*

Committee Member: *Franco Tassi*

Department Chair: *John S. Gierke*

For Science.

Contents

List of figures

List of Tables

Acknowledgements

I would like to thank my advisers, Chad Deering for his guidance, vast knowledge, sparking ideas, contagious endless motivation, personal kindness, sense of humor and especially for always (!) being there for me, helping immediately with even the smallest things and getting me back on track when I started to miss the forest for the trees, and Severine Moune for setting up the connections to Italy, the organization of the project, her guidance through the French Masters system and the final writing process and her helpful feedback, Franco Tassi and Francesco Capecchiacci for field support, the turbo-short course in fluid geochemistry, never ending explanations and for welcoming me kindly in their lab in Florence, and of course Samantha Fentress and Henriette Bakkar for helping and learning with me in the field and keeping my nerves together, especially Samantha for her endless positive spirit and good mood and Henriette for her good will and continuous help with "Costa Rica"-questions.

Many thanks to Waldo Taylor, Guillermo Alvarado, Chico and Orlando from ICE for helping where possible, taking time to go into the field, answering my million questions and being so kind and welcoming to make my time in the happiest country on Earth so much more enjoyable.

A special thank you to the "soil gas group" Peipei Lin, Carlo Prandi and Cindy Werner for the support, discussions, guidance, feedback, questions (!) and time spent together in the lab – I would not have been able to get through this without you!

And finally, I would like to thank all my friends at Michigan Tech and in Clermont for incredibly fun and exciting times, exploring new parts of the world together, motivating and distracting me in the everyday research life, complaining and being excited with me and of course for all the nonsense and laughs. Last but not least, I thank my family and friends at home that receive me lovingly every time I go home as if I was never away and that support me from afar.

Pura Vida!

List of abbreviations

CDP	Cumulative probability plot
ICE	Instituto Costarricense de Electricidad
IW4	Injection Well 4
LH	Las Hornillas
LOD	Limit of Detection
LP	Las Pailas
SCCM	Standard cubic meters per minute
sGs	Sequential Gaussian simulation
VOC	Volatile organic component

Abstract

Volcanic gas emissions are an important key component for monitoring volcanic activity and magmatic input of carbon dioxide into the atmosphere as well as the assessment of geothermal potential in volcanic regions. Diffuse soil degassing of CO_2 at Rincón de la Vieja and Miravalles volcanoes, assessed with the commonly accepted accumulation chamber method, showed the concentration of gas emissions in evident hydrothermal surface features in secondary gas emission zones of the volcanoes. Analyses of fumarolic gases were conducted to investigate similarities and differences between the volcanoes and the possibility of continued magma injection into their source(s). An output of 135 t/day over two degassing areas of together roughly 2 km^2 was calculated at Miravalles and one area of 0.129 km^2 at Rincón de la Vieja with 3.3 t/day. Comparatively low flux values and the particular soil flux distribution at the active Rincón de la Vieja volcano, suggests a different degassing behavior and stronger concentration of gas emissions at the active vent areas, compared to the dormant Miravalles volcano in case of a common hydrothermal reservoir. Similar chemical signatures of discharged fluids by the volcanoes of the Guanacaste region suggest a common hydrothermal reservoir fed by one or more magmatic source(s) with relatively primitive composition at Tenorio and Miravalles compared to Rincón de la Vieja.

Key words: carbon dioxide; degassing; Miravalles; Rincón de la Vieja; fluid chemistry; Costa Rica

1. Introduction

Carbon dioxide emissions into the atmosphere have recently been of interest due to the debate on natural vs. anthropogenic sources in the process of global warming. This has led to extensive research in a variety of fields to improve the accuracy of these estimates. Consequently, *The Deep Carbon Observatory (DCO)*, a large international collaboration was established, in order to evaluate natural input of CO_2 into the atmosphere. Active and dormant volcanoes are considered to be one of the major contributors to the global CO_2 gas emissions

The characterization of volcanic degassing is an important step to assess any volcano's state of activity and, therefore, its hazard potential. In general, a change in physical and chemical degassing behavior can indicate a change in the magmatic system and, therefore, the onset of a possible period of unrest or magma movement in the subsurface (Giggenbach, 1987).

Carbon dioxide emissions serve as a reliable tracer of magmatic activity due to its high abundance in magmatic gases (second most abundant species after H_2O) and its early escape from the magma due to its low and pressure-dependent solubility in the magma compared to other magmatic gas species (Gerlach and Graeber, 1985). Previous studies (e.g. Arpa et al., 2013; Brusca et al., 2004; Melián et al., 2014; Vaselli et al., 2010; Williams et al., 1986) have shown short-term changes in CO_2 degassing of volcanoes during the onset of a period of unrest related to magma movement and injection into the shallow storage system, which also correlates with seismic activity.

Gas emissions of volcanic systems have been shown to be concentrated in vents and fumaroles, but a significant portion also escapes through diffuse soil degassing (Allard et al., 1991; Baubron et al., 1990). The same has been found for hydrothermal/geothermal systems (in many cases due to past magmatic activity) and reservoirs created by thermal decomposition of sediments (Lewicki et al., 2007). These areas of diffuse soil degassing [Diffuse Degassing Structures (DDS)], firstly described by Chiodini et al. (2001) are often linked to volcano-tectonic structures and fracture zones of the emitting volcanic or hydrothermal systems. Their main characteristic is high soil permeability, where the majority of the gas emissions can escape diffusely through the soil rather than being focused through a fumarole.

Studies on the relationship between plume activity and secondary diffuse degassing have been summarized by Notsu et al. (2006) and suggested an increased diffuse soil degassing associated with lower plume activity and, inversely, lower soil degassing in a state of increased plume activity for different volcanoes.

The analysis of the chemical composition of volcanic emissions from the soil and surface degassing features (fumaroles, hot pools, etc.) is an important part of volcano monitoring and hazard assessment. Compositional changes and gas flux rates in fumaroles and bubbling pools can indicate magma movement, injection into the reservoir(s) and the onset of periods of unrest. Long-term chemical monitoring is used to study the evolution of volcanic systems. Furthermore, a possible link between adjacent volcanoes can be investigated by the comparison of the chemical compositions of their gas emissions. The study of linked volcanic systems could give information about their influence on each other and the possibility to detect regional magma movement in the subsurface and therefore potential volcanic activity. Finally, certain gas species emitted by volcanoes can provide insight into temperature conditions in hydrothermal systems (e.g. Giggenbach and Soto, 1992; Giggenbach, 1995; Tassi et al., 2005).

It has been shown that elevated diffuse soil emissions of CO_2 are frequently correlated with elevated soil temperature, and, therefore heat flow in volcanic and geothermal soil (Bloomberg et al., 2014; Chiodini et al., 2005; Werner and Cardellini, 2006; Werner et al., 2008). In recent years, workers have used diffuse CO_2 emissions as a tool for the calculation of heat flow in active geothermal regions of interest for exploiting the energy resource (Bloomberg et al., 2014; Fridriksson et al., 2006). Studying diffuse degassing in geothermally exploited areas reveals the potential of the geothermal reservoirs and the possibility to increase exploitation. In addition, diffuse degassing studies, when combined with the assessment of $\delta^{13}C_{CO2}$ values of the uprising gas, can be useful for identifying 'blind' geothermal areas (Bloomberg et al., 2014; Werner and Cardellini, 2006).

Study motivation and objectives

This study focuses on the Guanacaste region in Costa Rica, which has been investigated by the Instituto Costarricence de Electricidad (ICE) since the early 1970's and is thought to have vast geothermal potential. Two of the three volcanoes (Miravalles and Rincón de la Vieja) in the region are currently used for geothermal electricity production, while the potential for using the third volcano (Tenorio) is being explored. In addition, these volcanoes are surrounded by several communities and cities that could possibly be directly or indirectly affected by their activity.

No studies of diffuse soil flux of CO_2 have been conducted in the Guanacaste region with the exception of one large-scale study on Miravalles volcano by Melián et al. (2004). They investigated the flux over the entire volcano, although with few irregularly spaced measurement locations, which lead to large errors in flux estimates and, possibly, an overestimation of the total CO_2 output for the volcano. Therefore, a more detailed study of gas emissions from DDSs in the Guanacaste region is necessary to develop a foundation for a more reliable and thorough assessment of CO_2 emissions.

Furthermore, only a few studies on the geochemistry of volcanic fluids have been conducted in the Guanacaste region, mainly on Miravalles and Rincón de la Vieja (Gherardi et al., 2002; Marini et al., 2003; Tassi et al., 2005). At Tenorio, only preliminary results (Vaselli et al., 2003) on fluid discharges are available since Giggenbach & Soto's comparative study in 1992 on the whole Guanacaste volcanic region. They suggested that the three central volcanoes of the Guanacaste region, namely Rincón de la Vieja, Miravalles, and Tenorio, have a common hydrothermal reservoir feeding their hydrothermal surface features. Rincón de la Vieja is the most active center and Tenorio lies more in the periphery of this activity. Since 1992, sampling techniques for volcanic fluids have significantly improved (Montegrossi et al., 2001; Vaselli et al., 2006), facilitating more detailed analyses and more reliable values for volcanic gas species today. Consequently, additional data has been added to the previous database of volcanic fluid compositions to investigate their chemical composition.

The following is a list of scientific questions that were used to guide this study:

- What is the total CO_2 flux emitted into the atmosphere by these volcanoes?
- Do all three volcanoes share the same geothermal reservoir? Or does each operate independently?
- Does the diffuse degassing behavior correlate with the differences in volcanic activity recorded for each volcano?
- Is there more geothermal potential in the Miravalles geothermal field, currently unused by Costa Rica's electricity company? And, is this method for heat flow calculations derived from CO_2 emissions applicable in this region?
- What is the background emission of CO_2 by these volcanoes while in a state of quiescence?

2. Geological Setting of the Guanacaste Volcanic Region

The Guanacaste volcanic region forms together with the Cordillera Central the Costa Rican part of the Central American Volcanic Belt. This volcanic arc formed due to the subduction of the Cocos plate under the Caribbean Plate.

Most of Costa Rica lies on the Panama block, a microplate between the Cocos, Caribbean, Nazca and South American Plates, creating a complex setting of subducting plates and a center for volcanic activity [Fig. 1, after Kellogg and Vega (1995)]. The Guanacaste region is situated in the NW of Costa Rica, trending NW-SE, including five stratovolcanic complexes: 1) Orosí, 2) Rincón de la Vieja, 3) Miravalles, 4) Tenorio and 5) Arenal (Fig. 2). These volcanic complexes sit on top of a Tertiary basement divided into two complexes: the Guanacaste-Ignimbrite Plateau, formed between 8 and 1.6 Ma in a sequence of large explosive events alternating with repose periods, and the Arenal-Tilarán Plateau, produced by a long period of effusive volcanism between 2 and 1 Ma (Gillot et al., 1994).

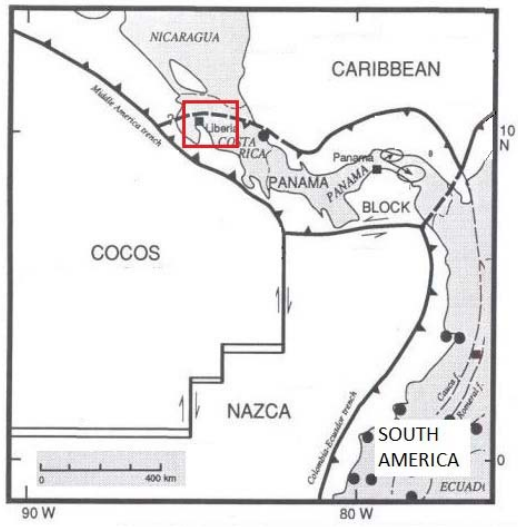

Fig. 1, Tectonic setting of the Central American Volcanic Belt with the Panama Block between the Cocos, Caribbean, Nazca and Southamerican Plates and the locationof the Guanacaste volcanic region in Costa Rica (red box) (modified from Kellogg & Vega 1995)

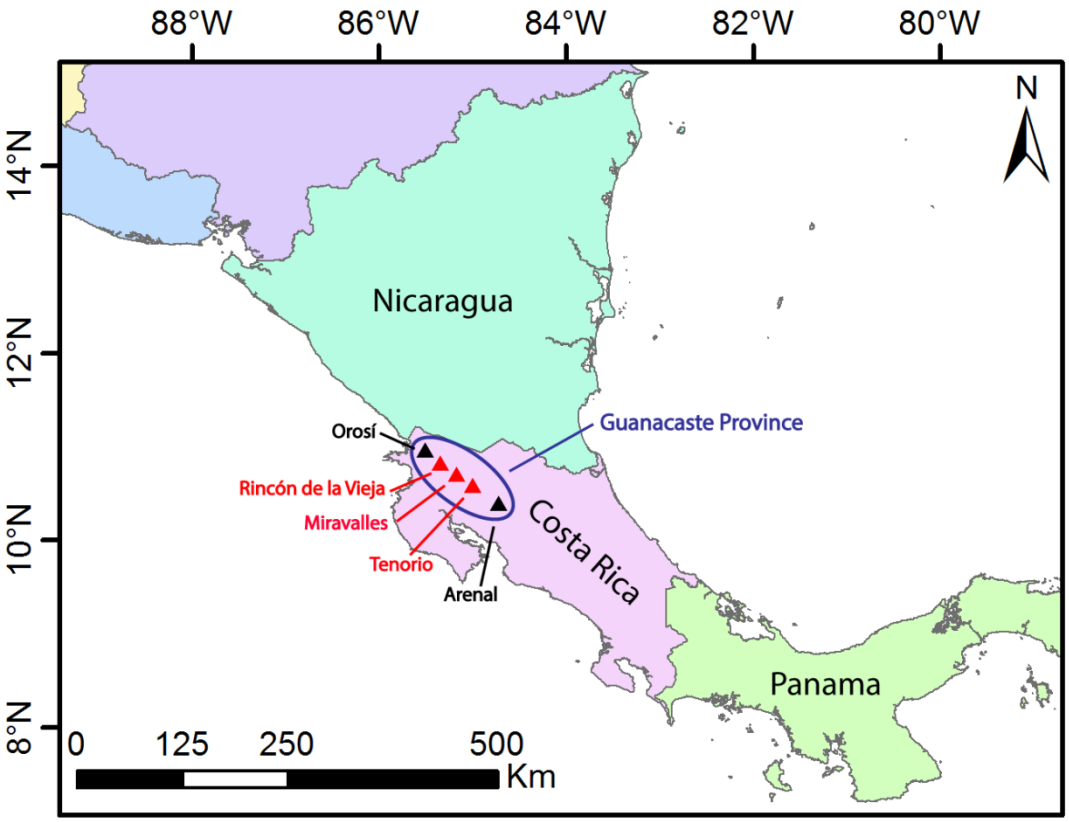

Fig. 2, Location of the Guanacaste volcanic region and the three studied volcanoes Rincón de la Vieja, Miravalles and Tenorio, Costa Rica

This study focuses on the three volcanic complexes in the center of the Guanacaste region, namely Rincón de la Vieja, Miravalles and Tenorio, suggested to have a common magmatic source due to petrologic (Chiesa et al., 1994) and fluid compositional similarities (Giggenbach and Soto, 1992). However, regional heterogeneities among the volcanoes are required to explain the vast range in silica content (Chiesa et al., 1994).

2.1 Miravalles

Miravalles is a stratovolcano and one of five cones of the Miravalles volcanic complex, lying inside the older Guayabo caldera. This caldera has a complex history of building the Guayabo volcano between 1.17 and 1 Ma and finally collapsing multiple times between 0.68 and 0.62 Ma with decreasing eruption energy towards the end (Alvarado and Gans, 2012; Chiesa et al., 1992). After the collapse of the caldera, intra-caldera activity built up a new stratovolcanic complex between 0.57 and 0.28? Ma, named Cabro Muco (Paleo-Miravalles). Finally, the volcanic complex

was completed by the creation of Zapote and Miravalles (Neo-Miravalles) volcanoes, the latter being the center of the last eruption ejecting juvenile material about 8000 years ago (Alvarado and Gans, 2012; Smithsonian, 2015a). The last and only historical eruption was a small steam explosion in 1946 (Smithsonian, 2015a). Today, the volcano is in a dormant state and shows only hydrothermal activity in various regions around its base, one of them being the fumarolic fields called "Las Hornillas" (Smithsonian, 2015a). This area around the surface expressions of the hydrothermal system has been found to be feasible for geothermal exploitation by the ICE and is now used for electricity production with three geothermal power plants, Miravalles I, II and III, with a total production design of 163 MWe (Moya and Yock, 2005).

2.2 Rincón de la Vieja

Rincón de la Vieja is a complex edifice of several volcanic structures. The paleo-volcanic Alcántaron formed between 2.16 and 1.78 Ma, when it finally collapsed, creating the associated Alcántaron-Guachepelín-Canas caldera after a series of minor collapses. Following this collapse, a series of dome growth and – collapse episodes took place before 1.6 Ma, when the complex of Proto-Rincón started growing. This volcano collapsed at 1.43 ± 0.09 Ma, forming the Canas Dulces caldera with a large eruption of 200 km^3 of rhyolitic material (Molina et al., 2014). The youngest members of the volcanic complex, Paleo- and Neo-Rincón, also known as the Rincon de la Vieja-Santa Maria complex, were dated from 0.56 Ma to present (Alvarado and Gans, 2012).

Rincón de la Vieja is the only active volcano in the Guanacaste volcanic complex and its last major eruption was of Plinian style and occurred about 3500 BP. Explosive Plinian eruptions and voluminous lava flows were part of Rincón de la Vieja's prehistoric activity (Kempter et al., 1996). After 3500 BP, the activity until today is characterized by mainly phreatic-phreatomagmatic eruptions with periodic pyroclastic flows and lahars, primarily on its NE side, towards the Caribbean Sea. Active periods have been found to last 5 – 7 years, reoccurring every 40 ±10 years (Soto, G. J., Alvarado, G. E., Goold, 2003). The lava is dominantly basaltic-andesitic in composition, but also including dacite and rhyolite. The Active Crater is the center of today's activity, hosting a hyper-acidic crater lake (with values toward pH 0) (Kempter and Rowe, 2000; Tassi et al., 2005), where all historical eruptions originated from (Smithsonian, 2015b).

2.3 Tenorio

The history of Tenorio volcano is still not very well known due to the lack of outcrops and its heavily vegetated surface. Evidence has been found of an old volcanic edifice called Monteverde and its construction was dated between 2.17 and 1.92 Ma (Alvarado and Gans, 2012). After a period of quiescence the new Tenorio volcanic edifice with several cones and active centers was built up in three major effusive phases, the first 0.74 – 0.54 Ma, the second 0.37 – 0.26 Ma and the third starting at 0.09 Ma (Alvarado and Gans, 2012). The complex is comprised of three distinct volcanoes, namely Tenorio, Montezuma and Carmela with the first being the most recently active one (Kitchen, 2002). Eruptive material was identified as basaltic-andesite to andesite (Kitchen, 2003). There is no evidence of an eruption in the Holocene and the volcano is designated as dormant (Smithsonian, 2015c). The volcano shows slight hydrothermal activity on its flanks, mainly as hot gas bubbling through rivers (e.g. surface expression "Borbollones" and "Hervideros") and bubbling hot pools (e.g. "Tierras Morenas"/"Alto Masís"). Seismic activity at Tenorio (and the Miravalles area) was recorded in October 1997 and 1998, which was thought to be related to tectonic activity of the NW-SE and NE-SW trending regional fault systems, rather than volcanic activity (Barquero and Taylor, 1998).

3. Description of the study areas and field work

3.1 Miravalles

At Miravalles, two study sites were investigated. The first, called the "Las Hornillas" (LH) area is part of the area actively used for geothermal exploitation (Fig. 3). It is the biggest investigated area at the base of Miravalles volcano, situated around visible surface expressions of the volcanoes hydrothermal system. Several clusters of non-vegetated, altered ground (1 – 1400 m^2) with fumaroles, boiling (mud) pools, frying pans and elevated soil temperature can be found in the LH study area, where high diffuse soil flux of CO_2 was expected. Geothermal power plant facilities are distributed over the whole area and outside of the obvious hydrothermal surface expressions. The volcano's flanks and base are covered in dense vegetation and tropical dry forests, having created a thick layer of soil with a significant amount of biogenic material; possibly creating diffuse CO_2 emissions from the soil with their decay. Clearings are either artificial or of hydrothermal nature, where elevated soil temperature and exhalation of significant amounts of CO_2 causes the death of vegetation. This LH area with strong hydrothermal activity coincides with a regional fault trending NE-SW through the volcanic complex (Fig. 3).

A second area investigated for diffuse soil flux of CO_2 was the "Injection Well 4" (IW4), named after the present injection well of the geothermal power plant. ICE communicated problems with the injection, as well as escaping gases on the site and in the creek next to it. The investigated area lies next to the community of La Fortuna and is on the edge of the geothermal power plant area, about 3 km to the SSW from the LH area. It is surrounded partly by dense forest and mainly by farm land. Escaping gas has been observed in the creek and altered ground on the injection well site, but none outside.

3.2 Rincón de la Vieja

At Rincón de la Vieja, a series of interconnected fumarolic fields (1 - 100 m^2) called "Las Pailas" (LP) on the south flank of the volcano, near its base, were investigated. It includes altered grounds, fumaroles, mud pools, hot pools and frying pans, surrounded by dense tropical dry forest, similar to the LH area at Miravalles. At Rincón de la Vieja these altered areas could also be related to the regional fault system (Fig. 3).

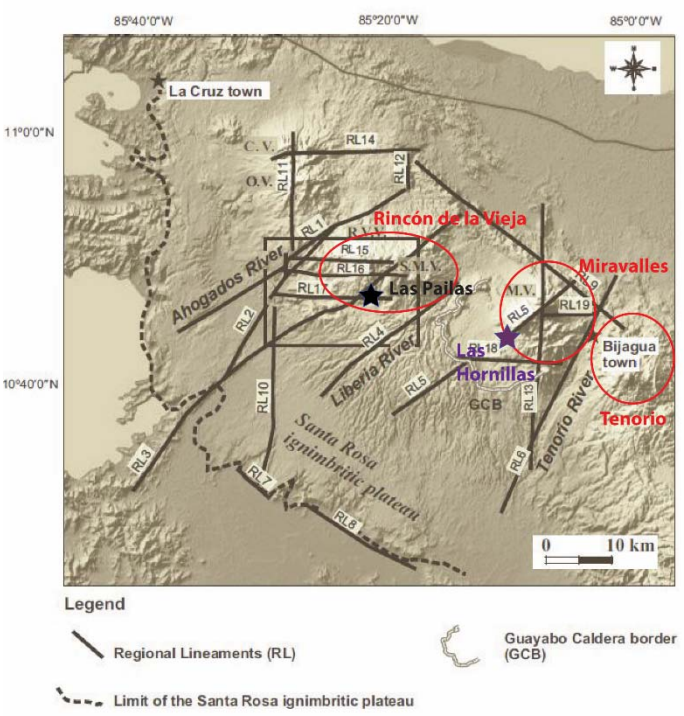

Fig. 3, Regional lineaments (faults and fracture zones) in the Guanacaste volcanic region and location of study areas for diffuse degassing surveys indicated by stars (modified from Molina et al., 2014, copyright-free publication)

3.3 Tenorio

Tenorio volcano is mainly covered by dense rainforest, creating soil of several meters thickness. Surface expressions of the hydrothermal systems are less obvious to find and often not connected to trails. Gas sampling was conducted in hot pools on its south flank and from gas bubbling through river water on its north side.

Field work

In January 2015 three weeks of field work were conducted in the Guanacaste volcanic region. Weather conditions in January are in general difficult and unpredictable in this part of Costa Rica, which lead to the complete abandonment of diffuse soil gas survey on Tenorio. High amounts of rainfall year round characterize the climatic circumstances around this volcano, saturating the soil with water and preventing diffuse transport of gas through the soil. For the same reason, the diffuse soil gas measurements were conducted at Miravalles and Rincón de la Vieja on dry days and avoiding days after heavy rainfalls, in order to analyze ideally undisturbed

gas flux from the deep reservoir and shallow biogenic input. A total number of 500 measurements were carried out at Miravalles and 134 at Rincón de la Vieja. The summit areas of both volcanoes were not accessible in this period, and therefore, no measurements could be taken from these areas and the degassing studies were focused on secondary gas emissions at the base of the volcanoes. Soil temperature maps were only created in the Las Hornillas and Las Pailas areas, where temperatures above ambient values were measured, while at the Injection Well 4 site, very uniform values were measured around ambient temperatures.

In addition to the diffuse degassing studies, gas samples from hydrothermal gas emissions were sampled over the course of several days. Most sampling locations were relatively easily accessible, while some required hours of driving and hiking through dense vegetation in strenuous conditions.

4. Methods

Various methods for the investigation of gas emissions in the Guanacaste region have been applied. In the LH area of Miravalles, all methods were used successfully, while in the other areas – due to weather conditions, material availability or lack of data – only some methods could be applied. The methods applied in each field survey location are summarized in Table 1**.**

Table 1 Summary of field surveys conducted in January 2015

Type of study	**Miravalles**		**Rincón de la**	**Tenorio**
Study areas	Las Hornillas	Injection Well 4	Las Pailas	-
Diffuse degassing maps	X	X	X	-
Soil temperature maps	X	X	X	-
Heat output estimate	X	-	-	-
Carbon isotopes from soil gas	X	-	-	-
Fumarole sampling	X	-	X	X

4.1 Diffuse soil gas flux

4.1.1 The principle of the accumulation chamber

The accumulation chamber technique has been widely used to quantify diffuse soil degassing of carbon dioxide and other gas species and confirmed as a valid technique to be applied in volcanic areas (Cardellini et al. 2003; Chiodini et al. 1998, 2001; Frondini et al. 2008; Lewicki et al. 2005; Notsu et al. 2006; Padrón et al. 2008).

The portable diffuse flux meter designed by West Systems S.r.l. used in this study, consists of: (1) handheld accumulation chamber with an integrated mixing device, (2) LICOR 820 infrared CO_2 gas analyzer and a TOX-05 electrochemical H_2S gas analyzer and (3) palmtop computer to operate the instrument (schema and details on the instrument in Fig. 4 and Table 2).

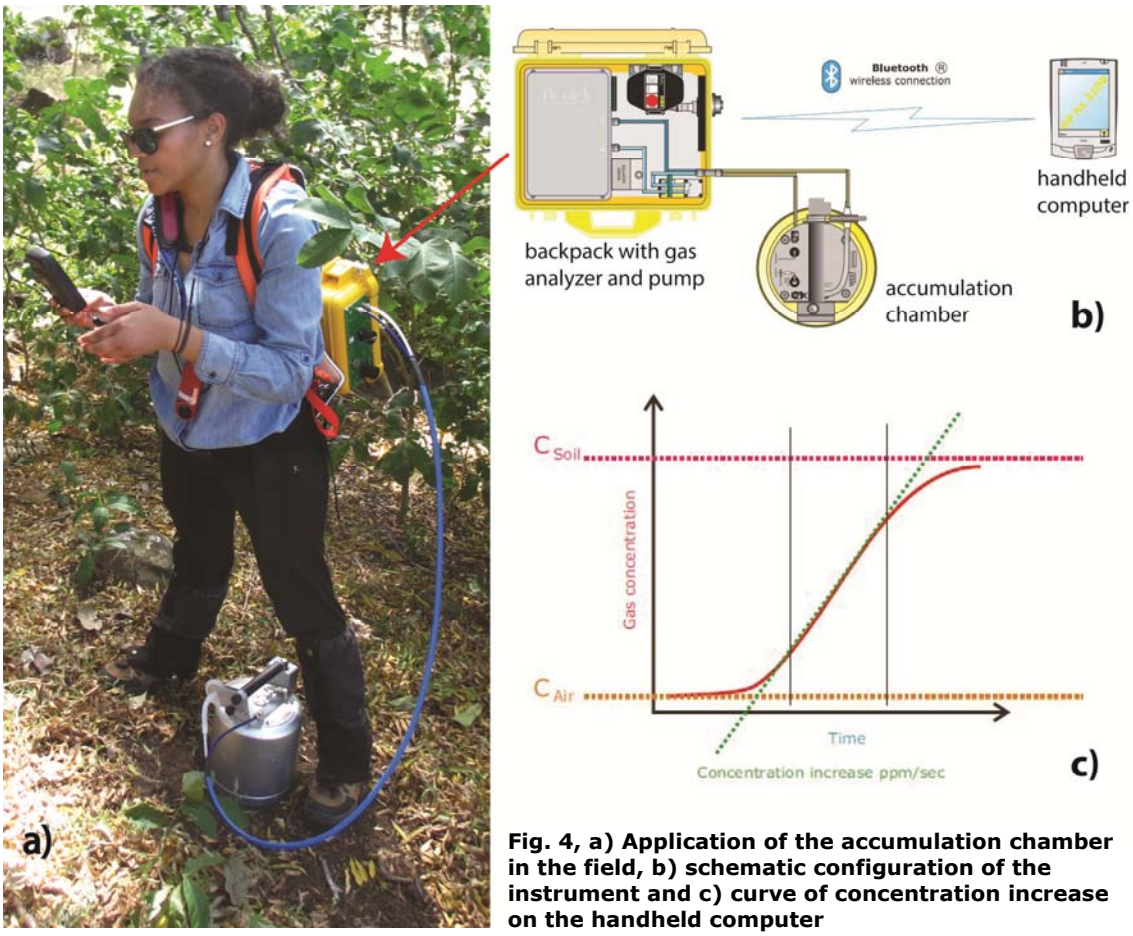

Fig. 4, a) Application of the accumulation chamber in the field, b) schematic configuration of the instrument and c) curve of concentration increase on the handheld computer

Table 2, Specifications for the West Systems accumulation chamber instrument

CO_2 analyzer	LI-COR 820
H_2S analyzer	TOX-05
Chamber type	B
Chamber volume	0.006186 m^3
Chamber footprint	0.0314 m^2
Pump strength	1000 SCCM

For each measurement, the accumulation chamber is placed on the soil and the measurement is started through the handheld computer after activating the integrated mixing device in the chamber. At each measurement point, a secure seal around the rim of the accumulation chamber on the soil has to be ensured in order to avoid the interference of atmospheric gases. The measurement lasts between 90 and 180 seconds or more if the curve was not stable enough in this time, in which the concentration of CO_2 in the chamber will increase. The fan in the chamber ensures the constant mixing of the captured gases and their even distribution. The pump transports the gas to the gas analyzers to measure the increase in concentration of CO_2 every second. This increase in concentration is reproduced as a curve on the handheld computer and the slope of this increase (ideally steady) is used to calculate the flux in ppm/s (Fig. 4c).

The barometric pressure and air temperature have been proven to influence the soil gas flux significantly (Hinkle, 1994) and, therefore, they have to be included into the calculation of the real gas flux. Laboratory experiments by Chiodini et al. (1998) showed that by injecting a constant known gas flux through a soil sample under different barometric pressure conditions, a negative correlation exists between barometric pressure and CO_2 flux. The barometric pressures are recorded by the instrument at each measurement and air temperature measurements were conducted manually for later corrections of the flux values.

4.1.2 The application of the accumulation chamber in the field

Carbon dioxide flux measurements were conducted at three different geothermal environments on the Miravalles and Rincón de la Vieja volcanoes. Due to heavy vegetation, the distribution of the measurement points is irregular; the spacing at the "Las Hornillas" area varied between 5 and 200 m, at the "Injection Well 4" site between 30 and 70 m and at the "Las Pailas" area between 10 and 80 m. The spacing was kept closer in areas of high soil flux and visible ground alteration, in order to maintain a high level of detail in the regions of significant CO_2 output from the volcanic hydrothermal systems. The lack of vegetation in high alteration zones favored the more detailed investigation. Greater spacing was applied in the areas distant from the high flux zones, fracture and fault zones, where "background" flux was measured and in very strongly vegetated areas. Thick vegetation was one of the main causes of an irregular measurement grid and can also be a possible reason for enhanced CO_2 production in the soil, contributing to the total measured flux.

Soil temperatures were measured at 10-15 cm depth with a thermocouple and a digital thermometer within a 0.2 m radius from the accumulation chamber footprint. Air temperature, humidity and wind speed were determined at each flux measurement location. Wind speeds varied significantly between 0 and 20 km/h and occasionally up to 46 km/h, creating a possible source of variation in the measured soil fluxes, as well as the variation of the relative humidity at different sampling sites. Quantification of the influence of these factors was not possible in this study.

4.1.3 Data analysis

The gas flux measurements were converted from ppm/s to g/m^2/day, taking into account the volume and footprint of the accumulation chamber and including the air temperature and barometric pressure taken at each measurement. The conversion factor *K* is calculated with the following formula:

$$K = \frac{86400 * P}{10^6 * R * T_K} * \frac{V}{A} \quad (1)$$

where *P* is the barometric pressure in mbar, *R* the ideal gas constant (0.08314510 bar*L/K/mol), T_k the air temperature in Kelvin degree, *V* the chamber volume in m^3 and *A* its footprint area in m^2. The flux in ppm/s is multiplied by the conversion

factor K to obtain a flux in moles/m^2/day, which is again multiplied by the molecular weight of CO_2 (44.01 g/mol) to obtain g/m^2/day.

The carbon dioxide flux and soil temperatures were then statistically analyzed for their distribution and correlations. Values of CO_2 flux under the limit of detection (LOD, 0.44 g/m^2/day, D. Continanza, West Systems®, personal communication) were substituted with a value of 0.311 g/m^2/day. This value corresponds to the LOD/√2, which is, according to Croghan and Egeghy (2003) and Verbovsek (2011), the best-fitting substitution method to include values under the LOD.

The distributions of the individual data sets were evaluated as a first step of exploratory data analysis. In case of a bimodal or polymodal distribution of the data, it is important to distinguish among the different populations in the gas flux or soil temperature data sets. The most reliable tool for this is the cumulative probability plot (CDP) technique, according to A.J. Sinclair (1974) and Harding (1949). With this technique, data populations are separated at inflection point(s), where the curvature of the CDP curve changes its sign (concavity), based on the assumption that the data set is either normally or log-normally distributed, which has to be confirmed with a histogram and/or QQ plot before the procedure. This CDP technique allowed for background and peak flux/temperature populations and in some cases an intermediate population (e.g. the "Las Hornillas" area in this study, see "Results" section) to be identified.

For the calculation of the total output of CO_2 for the study areas, non-sampled points in the areas were simulated by using the sequential Gaussian simulation (sGs) method. This method has been shown by Lewicki et al. (2005) and Cardellini et al. (2003) among others to be an effective and precise method for the interpolation of diffuse soil degassing, providing not only a highly detailed map of fluxes, but also facilitating the calculation of the range of total flux over all the conducted simulations. The sGs takes the spatial auto-correlation of the data into account and models each unknown point in the grid using the surrounding measured neighbor points and the previously modeled cell. Therefore, a semi-variogram model, based on the empirical semi-variogram of the dataset, is used as an input model for the simulations. Detailed descriptions of the processing in the GSLIB software are provided by Deutsch and Journel (1998). The total CO_2 flux of the study areas was

calculated by multiplying the value of each simulated CO_2 flux cell with the area it represents and summing the simulated flux across the grid.

The same method of interpolation was applied to the soil temperature measurements to produce maps of the soil temperature over the whole study areas. Input parameters for the different simulations are specified in Table 3.

Table 3, SGs input parameters for the interpolation of CO_2 and soil temperature at the different study areas

	Empirical variogram		**Variogram model**			**sGs**	
Study area + measurement type	**lag distance [m]**	**lags tolerance**	**nugget**	**range [m]**	**variogram type**	**# of simul.**	**grid spacing [m]**
LH CO_2	20	15	0.1	70-100	exponential	1000	5
LH soil T	25	15	0.05	110-160	exponential	1000	5
IW4 CO_2	40	20	0.1	210-260	Gaussian	700	1
LP CO_2	25	13	0.9	50-80	spherical	1000	5
LP soil T	20	10	0.4	30-45	spherical	1000	1

4.1.4 Calculation of mass and heat flow from CO_2 flux

Steam, and subsequently heat flow, can be estimated by using the $[H_2O]$:$[CO_2]$ ratio from fluids derived from the deep hydrothermal system and multiplying it by the total CO_2 output of the system (e.g. Bloomberg et al., 2014; Fridriksson et al., 2006)

$$F_{stm\,(CO2)} = F_{CO2\,tot} * \frac{[H2O]}{[CO2]} \quad (2)$$

where $F_{stm\ (CO2)}$ is the steam mass flow in g/s, $F_{CO2\ tot}$ is the total CO_2 output of the investigated area (converted from t/day to g/s) and $[H_2O]$ / $[CO_2]$ is the mass ratio. Selected high-CO_2-flux areas of the LH area were used to calculate the $F_{CO2\ tot}$. A $F_{CO2\ tot}$ of 30.64 t/day was calculated for these selected high flux areas by summing up significant portions ("hotspots" in the CO_2 flux results map, Fig. 8) of the simulated CO_2 map, which could possibly depict areas where magmatic CO_2 reaches the surface and could, therefore, be representative of the uprising magmatic-hydrothermal gas in the subsurface. $[H_2O]$:$[CO_2]$ mass ratios of two different wells (Pozo 11 = 24.16 and Pozo 63 = 83.47) were used to calculate a range of possible steam flow rates. Subsequently, the heat output of the selected high flux areas was calculated in the following way:

$$Hs = F_{stm\,(CO2)} * hs_{97.5°C} \quad (3)$$

where Hs is the heat output in kJ/s or W and $hs_{97.5°C}$ is the enthalpy of H_2O at 97.5°C (2671.6 kJ/kg), which corresponds to its boiling point at 700 m a.s.l. (average elevation of the LH area). The heat output of the high flux zones was then extrapolated over the whole power plant area to evaluate the heat flow in the subsurface derived from the CO_2 flux at the hotspots and in order to draw a comparison to the power plant production capacity. This was only possible in the Las Hornillas area on Miravalles, due to the availability of previously collected unpublished data for $[H_2O]$:$[CO_2]$ ratios in gas emissions of wells in this area.

4.2 Gas geochemistry

4.2.1 Geochemical sampling of fumaroles/hot pools

4.2.1.1 Sampling method for major gas constituents

Gas samples were taken from surface expressions of the different hydrothermal systems of the three volcanoes, e.g. fumaroles and bubbling hot pools at Tenorio, Miravalles and Rincón de la Vieja volcanic complexes. In order to analyze the major and minor constituents of gases escaping from fumaroles and hot pools, a method of sampling has to be applied which ensures the least amount of air-contamination and post-reaction of the gas to preserve its original composition. This is accomplished with the method of Montegrossi et al. (2001) using a pre-weighted and pre-evacuated 50 mL thorion-tapped glass tube, filled with 20 mL of purified 0.15M $Cd(OH)_2$ in 4 M NaOH, as a refinement of the method of Giggenbach (1975).

Since only low temperature emissions (T < 100 °C) were sampled, a plastic funnel could be used to focus the emission, which was placed upside-down and secured over the gas emission (fumarole or bubbles rising in a hot pool), fully covering it, in order to capture the full emission and to avoid as much air contamination as possible. The vial with the cadmium-soda solution was placed on the rubber tube connection on the funnel and opened after securing it to slowly let the volcanic gases accumulate (Fig. 5).

Fig. 5, Sampling apparatus with flask for major gas constituents

The solution in the flask absorbs CO_2, HF, HCl and SO_2 (as SO_3^{2-} and SO_4^{2-}) while H_2S precipitates as CdS by reacting with the $Cd(OH)_2$, slowly turning the solution yellow. This precipitation prevents the reaction of SO_2 and H_2S ($2\ H_2S + SO_2 = 3/x\ S_x + 2\ H_2O$) during and after sampling, in order to analyze their original abundances. Incondensable gases (e.g. O_2, H_2, CO, COS, CH_4), noble gases (e.g. Ar, He, Ne) and other hydrocarbons move through the solution and accumulate in the flask's headspace. Sampling lasts until the pressure in the headspace of the vial is equal to the pressure of the sampled gas emission.

4.2.1.2 Sampling for CO_2 isotope analyses and volatile organic components (VOCs)

In order to sample volcanic gas for carbon isotope and VOCs analyses, separate flasks have to be used to capture the gas. VOCs would immediately react with the alkaline solution in the flask for major constituents and new organic compounds, previously not present in the fumarolic gases, would form or previously present species would break up into other compounds. At each fumarole/steam heated pool, one flask was used for carbon isotopes and one for VOCs, by extracting gas from the funnel (same set up as with sampling for main constituents) with a syringe of 60 mL volume and injection into an evacuated vial (Exetainer®) of 10 mL volume, by piercing its semipermeable membrane in the cap with the syringe needle.

In addition to fumarolic gases, six samples of soil gas were taken directly from the accumulation chamber at Miravalles volcano, in order to investigate a possible correlation between CO_2 soil flux and the isotopic signature. This survey was aimed at distinguishing between magmatic and biogenic carbon dioxide sources in combination with the statistical method. Samples were collected from the top of the accumulation chamber by extraction with a syringe and transferred into the same type of vial (Exetainer®) at the end of each measurement of different flux rates, when enough CO_2 had accumulated in the chamber. Due to the limited number of flasks available in the field, not more than six samples could be taken at Miravalles and this survey could not be reproduced at Rincón de la Vieja.

4.2.2 Laboratory analyses of fumarolic gases and data treatment

Major and minor constituents of the collected gas samples, were measured over one week in the Laboratory of Fluid and Rock Geochemistry and the Laboratory of Stable Isotopes at the Department of Earth Sciences (University of Florence).

4.2.2.1 Main constituents and light hydrocarbons

The first part of the analysis of the gas captured by the flasks, containing the soda-cadmium solution, was the measurement of incondensable gases accumulated in the flask's headspace. Two different gas chromatographs are available in the laboratory of the Department of Earth Sciences (University of Florence) for this purpose. The Shimadzu 14A is used for the measurement of CO through methanization and hydrocarbons after the methods of Vaselli et al. (2006). Heavier hydrocarbon gases (C > 10) have to be analyzed through gas mass spectrometry (Capecchiacci, 2012).

Vaselli et al. (2006) furthermore provide a detailed description of the analysis of H_2 (> and < 5000 ppmv), Ar, He, Ne, O_2, N_2, CH_4 (>1000 ppmv) and CO (> 350 ppmv) through the Shimadzu 15A chromatograph (Fig. 6), containing a Flame Ionization Detector, with He, Ne or Ar as a gas carrier, depending on the analyzed species.

Fig. 6, Gas chromatograph Shimadzu 15A for the analysis of H_2, Ar, He, Ne, O_2, N_2, and CO content

The chromatography methods are all based on the fact that different chemical constituents react in a different manner with the stationary phase of the chromatograph. This causes the different constituents to arrive at the detector at different times and, therefore, to be distinguished from one another by their arrival times. Integrating the area under the different peaks can then be used for the calculation of the concentration of each species.

The precipitated and dissolved species in the solution can then be analyzed after the methods of Montegrossi et al. (2001). The solid and liquid phases were removed from the flask, transferred into Teflon centrifugation tubes by a water pump and centrifuged to separate the solid and the liquid phases. In the liquid phase the following species can be analyzed:

- Carbonatic species, from the dissolution of CO_2 , determined by titration with acidimetric volumetry,
- Cl^- , originally from HCl in the gas, analyzed by ion chromatography, and
- SO_4^{2-} (from dissolution of SO_2), also with ion chromatography.

The solid phase CdS is dissolved and re-centrifuged to eliminate Cd and total sulfur. The resulting SO_4^{2-} is used to analyze the H_2S concentration by ion chromatography. The final solid phase $Cd(OH)_2$ and elementary sulfur are separated and the elementary sulfur concentration is measured by ion chromatography with the SO_4^{2-} formed by its oxidation (Vaselli et al., 2006).

4.2.2.2 Carbon isotopes

To evaluate the origin of the CO_2 in the discharges of the hydrothermal system, the stable isotopic composition of the CO_2 in the sampled gas was analyzed ($\delta^{13}C_{CO2}$). To achieve this, the proportion of ^{13}C to ^{12}C in the CO_2 of the sampled gas is used. Therefore, the CO_2 has to be separated from the other constituents using a two-stage cryogenic trap.

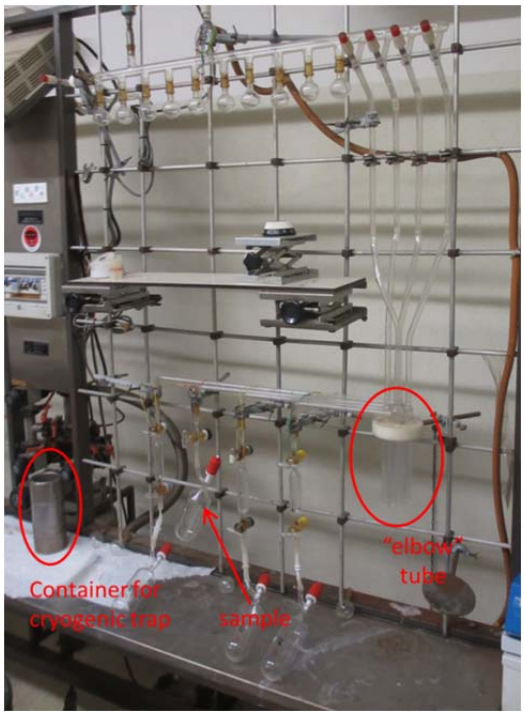

Fig. 7, Apparatus for separation of CO_2 from the sampled volcanic gas

Before this trap can be applied, it has to be determined by the gas chromatography method if H_2S is present in the sampled gas. The cryogenic trap cannot separate CO_2 from H_2S, because both of their boiling points are below the temperature of the second stage of the cryogenic trap, causing both of them to remain as a solid; therefore, if H_2S is present, H_2S has to be eliminated from the gas phase beforehand.

After the determination of the absence or the elimination of H_2S, the first stage of the cryogenic trap can be initiated. The vial containing the sampled gas is connected to one of the tubes of the trap transferred into its evacuated tube system. A container with liquid nitrogen (-190 °C) is installed to surround the "elbow" part of the tube. This causes H_2O and CO_2 to condensate and to gather in the lower part of the tube, while the other phases, still in gaseous state, are evacuated through the valve on the uppermost end of the system (Fig. 7).

After this first separation, the trap with liquid nitrogen is removed and the second cryogenic trap is applied. It contains a mixture of liquid nitrogen and trichloroethylene and is applied the same way as in the first trap. The now higher temperature causes the CO_2 to transform back into the vapor phase, while H_2O remains solid. This procedure ensures a concentration of 99.999 % CO_2 in the remaining gaseous phase, which is captured in a separate container for the following stable isotopic ratio analysis.

The analysis of the stable isotopic composition of the CO_2 was conducted with a mass spectrometer in the CNR (National Council of Research) – IGG (Institute of Geosciences and Earth Resources) of Pisa/Italy, where the ratio of mass over charge of the carbon in the CO_2 molecules was determined. Due to the higher weight of ^{13}C compared to ^{12}C, the ratio of these two isotopes can be calculated and is expressed in $\delta^{13}C_{CO2}$, by normalizing it to the Pee Dee Belemnite standard with the following formula:

$$\delta^{13}C_{\mathrm{Sample}} = \left(\frac{{}^{13}C/{}^{12}C_{\mathrm{Sample}}}{{}^{13}C/{}^{12}C_{\mathrm{PDB}}} - 1 \right) \cdot 1000 \qquad (4)$$

Several different sources of the soil CO_2 are possible, each having a unique signature of $\delta^{13}C_{CO2}$. These include mantle derived magmatic CO_2 [$\delta^{13}C_{CO2}$ = -8 to -3‰ (Hoefs, 1987)], CO_2 from organic soil respiration [$\delta^{13}C_{CO2}$ between -13 and -30‰ (Cerling et al., 1991; Keeling, 1961)], as well as from input of carbonate sedimentary rocks into the magmatic source [$\delta^{13}C_{CO2}$ = -1 to +4‰, (Faure and Mensing, 2005)] and contamination of the soil gas by atmospheric CO_2 [$\delta^{13}C_{CO2}$ = -6 to -8‰, (Cerling et al., 1991)]. Carbon isotopic values have been determined for all samples from fumaroles and steam heated pools and four of six samples from the accumulation chamber contained enough CO_2 for the analysis of $\delta^{13}C_{CO2}$ values.

Table 4, Summary of methods conducted for gas analysis

Analyzed component	**Method**
Incondensable gases (H_2, Ar, He, Ne, O_2, N_2, CO)	Gas chromatography
CO_2	Acidimetric volumetry
HCl, SO_2	Ion chromatography
H_2S, S_8^0	Ion chromatography
Light hydrocarbons (CH_4, C_2H_6, C_3H_8, C_3H_6, i-C_4H_{10}, n-C_4H_{10}, i-C_4H_8, C_6H_6)	Gas chromatography
H_2O	subtraction of analyzed species from sampled gas
$\delta^{13}C_{CO2}$	Gas mass spectrometry
R/Ra	Gas mass spectrometry

5. Results

5.1 Diffuse soil gas flux

5.1.1 "Las Hornillas" area, Miravalles power plant

The investigated area around the "Las Hornillas" fumarolic fields lies completely within the power plant's area of production and has an areal extent of 1.99 km^2. The measured CO_2 flux of 436 measurements in this area varied between below detection limit (0.311 $g/m^2/day$) and 11004 $g/m^2/day$, with an average of 253 $g/m^2/day$ and a standard deviation of 808 $g/m^2/day$ (Fig. 8). Fumarolic fields with high flux can be identified by "warm" colors in the map. Two areas of particular flux patterns have been identified. Zone A between the fumarolic fields and Zone B, inside an old quarry (Fig. 8).

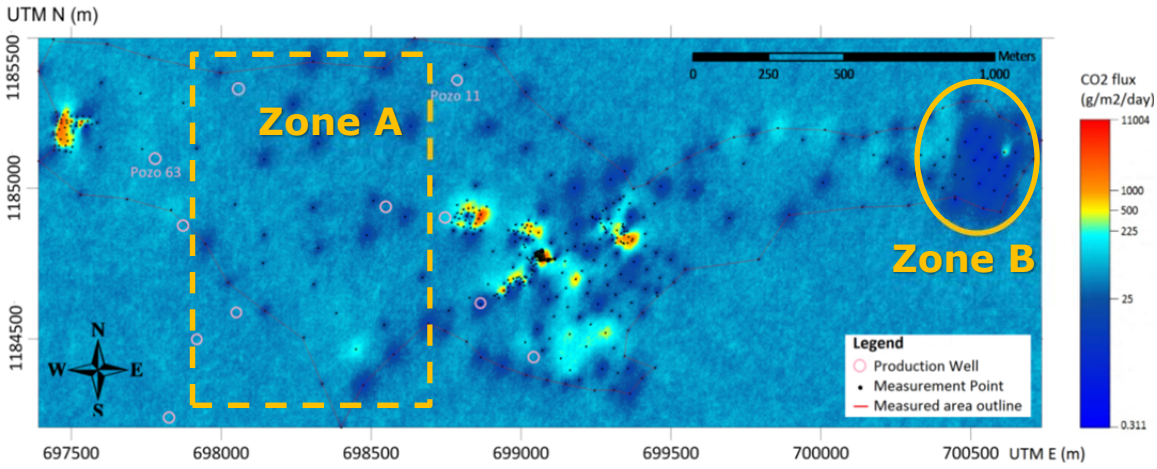

Fig. 8, Map of sGs results for CO_2 flux (logarithmic scale with the population break points of 25 and 225 $g/m^2/day$ and significant high values) for the investigated LH area (1.99 km^2). The thin red outline shows the area used for the calculation of the total CO_2 output, black dots indicate the measurement locations, pink circles production wells of the geothermal power plant, and Zone A and B in orange, which are areas of interest.

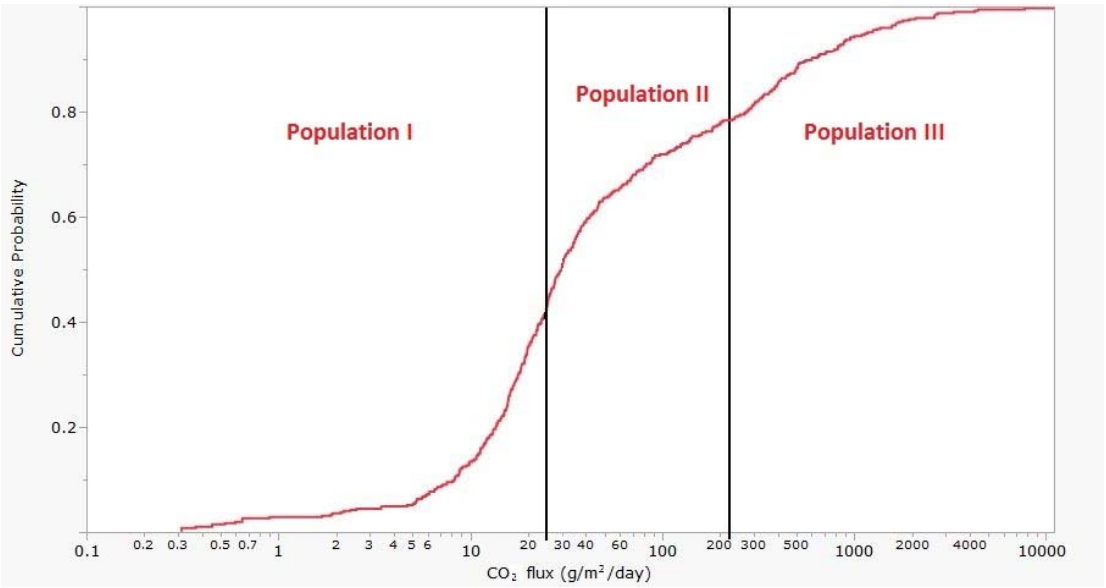

Fig. 9, CDP of the measurements in the LH area with population break points (black lines) at 25 and 225 g/m^2/day, where population I is the background, population II the mixed group and population III the peak

A representation of the CO_2 flux data in a cumulative distribution plot (CDP) (Fig. 9) shows the existence of three different populations of flux values, with population I ("background") ranging from the LOD to 25 g/m^2/day with a mean of 13 g/m^2/day, population II ("mixed") between 25 and 225 g/m^2/day with a mean of 64 g/m^2/day and population III ("peak") from 225 to the maximum value measured with a mean of 1044 g/m^2/day. The three populations make up 43.3 %, 35.1 % and 21.6 % of the data, respectively.

A total mean CO_2 output of 133 t/day was calculated, with a minimum of 118 and a maximum of 151 t/day in 1000 realizations (95 % confidence interval), which corresponds to a maximum error of 13.5 % of the total mean flux estimate. The zones with relatively high efflux (peak and/or mixed populations) of CO_2 through the soil are concentrated around the obvious surface expressions of the hydrothermal area, such as fumaroles and hot pools. These are surrounded by patches of altered grounds of varying size, estimated from 1 m^2 up to 200 m^2. They are characterized by the lack of vegetation and alteration of the soil minerals, causing a noticeable difference in soil color, ranging from light brown, to orange, to white. Outside of these non-vegetated areas, the CO_2 flux drops rapidly to background values (flux population I) or to slightly higher values in the range of the mixed flux population. A

very low flux area was observed in the very east of the study area (orange circle, Fig. 8), which is an old quarry and almost completely stripped of vegetation.

The best-fit semi-variogram, used to build a model for spatial correlation for the sequential Gaussian simulation of the CO_2 efflux and the soil temperature in the "Las Hornillas" area, are presented in Fig. 10. It can be observed that a spatial auto-correlation exists in the data (red points) until about 150 m distance for the CO_2 flux and until about 150 – 200 m for the soil temperature, where the variogram plateaus out, with points fluctuating around a variance value of 1. The models used (blue lines) for both the CO_2 flux and soil temperature are of the exponential variogram type, which was observed to be the best fit for this particular data set.

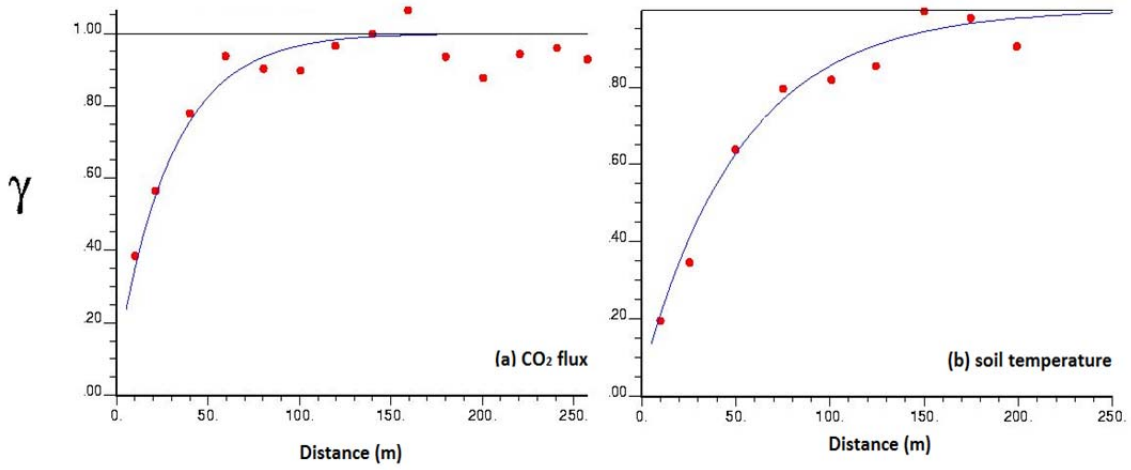

Fig. 10, Semi-variograms for sGs of a) CO_2 flux and b) soil temperature of the LH area, with horizontal distance of measurement points on the x-axis and γ for the variance on the y-axis, where a value of 1 corresponds to the total absence of spatial auto-correlation. Red dots represent the empirical semi-variograms and the blue lines the semi-variogram models

A positive logarithmic correlation of CO_2 efflux and soil temperature has been found in the area of the Miravalles power plant (Fig. 11), which is coherent with other soil flux studies in volcanic areas (Bloomberg et al., 2014; Werner et al., 2008). The simulated map for soil temperatures in the "Las Hornillas" area is presented in Fig. 12. Visual comparison of the CO_2 efflux and the soil temperature map shows a similar spatial variation of high values. The same similarity of the two data sets can be observed comparing the variograms showing a comparable spatial auto-correlation of the measurements. The soil temperatures in this area range from 19.4 to 97.7 °C with a mean of 32.0 °C and a standard deviation of 16.4 °C.

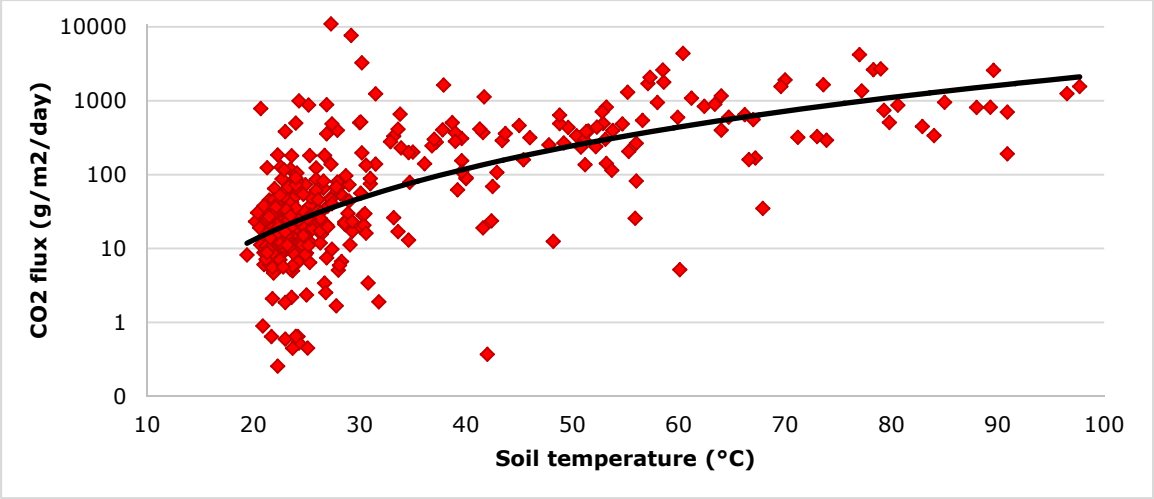

Fig. 11, Positive correlation (black line) of CO_2 flux and soil temperature in the LH area

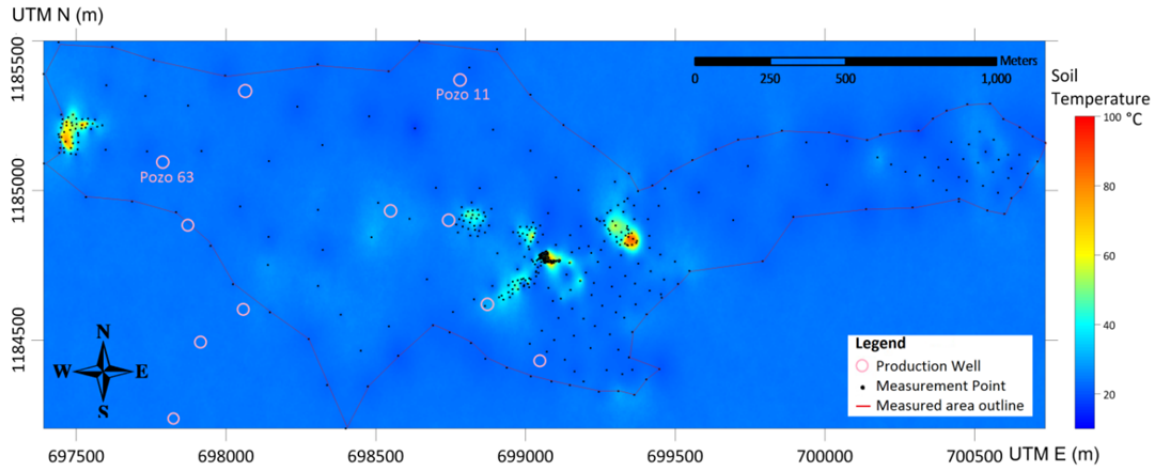

Fig. 12, Map of sGs results for soil temperature in the LH area, black dots indicate the measurement locations and pink circles the geothermal wells

Carbon isotopic values of soil CO_2 have been determined at four different flux rates in the Las Hornillas area of the Miravalles geothermal field (Fig. 13). There is no apparent correlation between carbon isotopes and the CO_2 flux rate. In previous studies (Bloomberg et al., 2014; Chiodini et al., 2008; Werner and Cardellini, 2006), positive correlations of $\delta^{13}C_{CO2}$ and CO_2 flux were determined in volcanic/hydrothermal areas, which could not be found in this study.

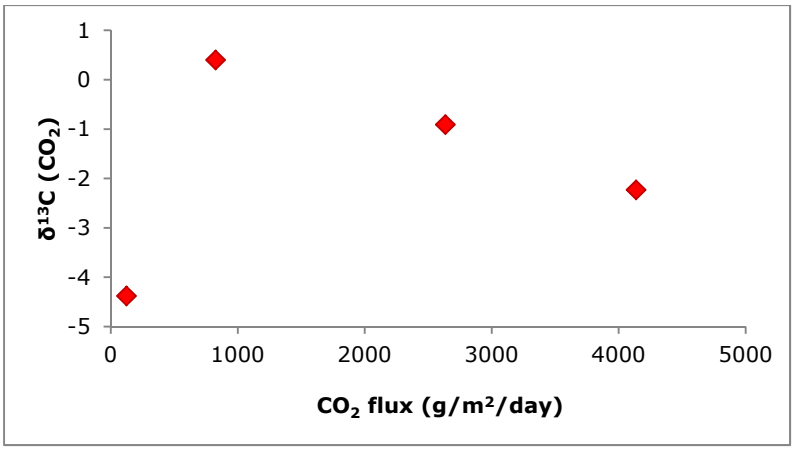

Fig. 13, CO_2 flux vs. $\delta^{13}C_{CO2}$ from accumulation chamber samples in the LH area

Steam mass and heat flow of the Miravalles power plant area

Discharges from two production wells (Pozo 11 and Pozo 63) were used to estimate the ratio of H_2O to CO_2 in the uprising fluids from the underlying geothermal reservoir at Miravalles volcano. This was only calculated in the LH study area, due to the availability of data of deep geothermal wells, showing a ratio of presumed deep origin. Chemical compositions of gases in fumaroles and steam heated pools show low abundances of H_2O due to condensation in shallow depths. Therefore, it was only possible to conduct this heat flow estimate at the LH area, where discharge data from wells was available.

Both wells that were used as an estimate of upflowing CO_2 are situated between the fumarolic fields of the LH area (visible in "warm" colors in Fig. 8). The distance from Pozo 11, which has a $[H_2O]:[CO_2]$ ratio of 24.16, to the nearest high flux field is about 400 m and the Pozo 63 lies about 270 m away from the next high-flux zone and has a ratio of 83.47, suggesting a higher $[H_2O]:[CO_2]$ ratio with decreasing distance to the main fluid upflow zones. The heat flow calculations, using equation 2 and 3, give a value of 22,896 W for the Pozo 11 ratio and 79,079 W for the Pozo 63 ratio for selected high-flux zones (total extent 95364 m^2). Extrapolation of these values to the whole geothermally used power plant area (16 km^2) yields heat flow values of 3.8 MW and 13.3 MW, for the two ratios, respectively. Compared to the production design of the power plant, which is around 163 MW, these values are significantly lower.

5.1.2 Injection well 4 site, Miravalles power plant

Carbon dioxide flux in the Injection Well 4 site varies between below the LOD and 385 g/m^2/day with a mean of 22 g/m^2/day and a standard deviation of 49 g/m^2/day among 64 measurements on an area of 0.172 km^2. The existence of two distinct populations is shown by the CDP in Fig. 14 with the inflection point at 14 g/m^2/day. The background population below this value represents 54.7 % of the data with a mean of 6 g/m^2/day, while the peak (above the inflexion point) represents 45.3 % with a mean of 39 g/m^2/day.

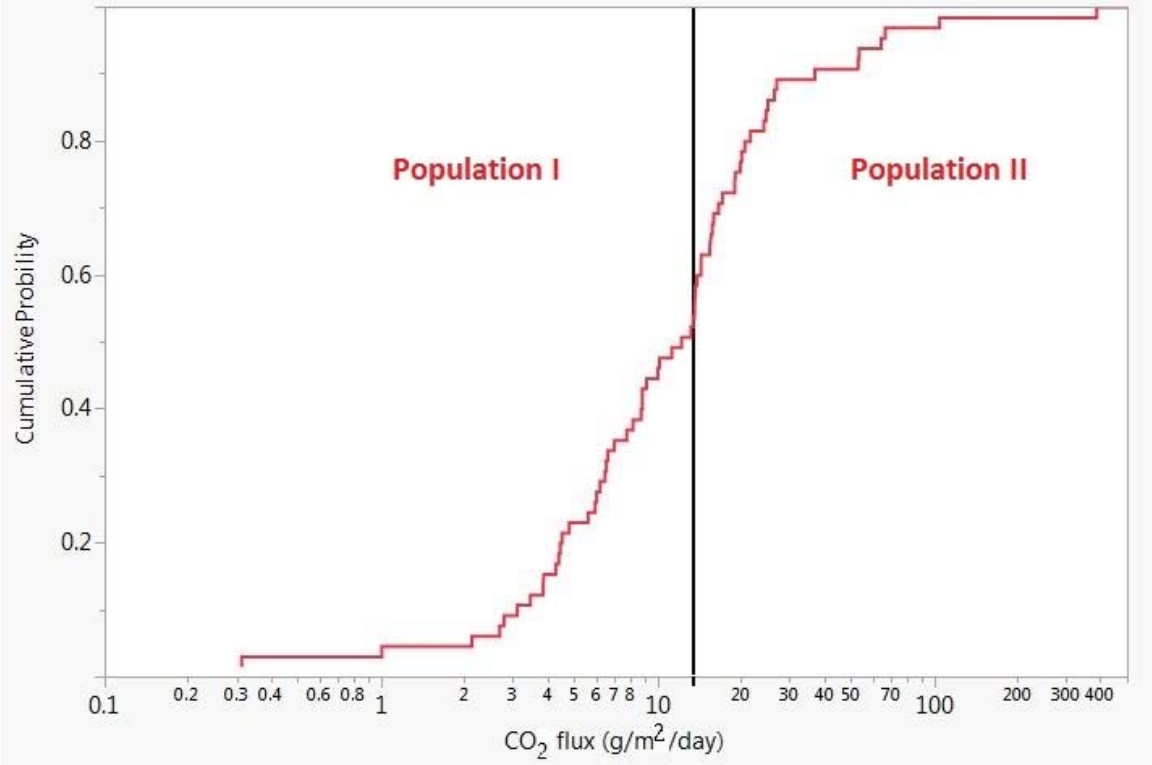

Fig. 14, CDP and histogram of the CO_2 flux measurements on the IW site with a break point at 14 g/m^2/day, separating background (population I) and peak (population II) flux

The empirical variogram and the variogram model used for the sGs show a clear spatial auto-correlation until about 300 m (Fig. 15b). A total mean CO_2 output of 2.2 t/day was calculated for the whole area around the injection well of 0.172 km^2 (Fig. 15a), with a minimum flux of 2.1 t/day and a maximum flux of 2.6 t/day in 700 realizations (95 % confidence interval). This corresponds to a maximum error of 15.8 % of the total mean flux estimate.

The highest value measured is not on the injection well site but in the middle of the adjacent meadow accommodating several wells observed during field work. The efflux value of 27 g/m^2/day, measured on the injection well site, lies above the background, but far from the highest measurements. Escaping gas from the soil through the water of the creek was observed next to the injection well site, where the second largest CO_2 soil flux was measured. Some m^2 of altered ground was observed and a strong odor of H_2S was present on and around the injection well site. Soil temperature on this site was slightly elevated with 33°C (maximum value in this area), while all other measurements were around ambient temperatures.

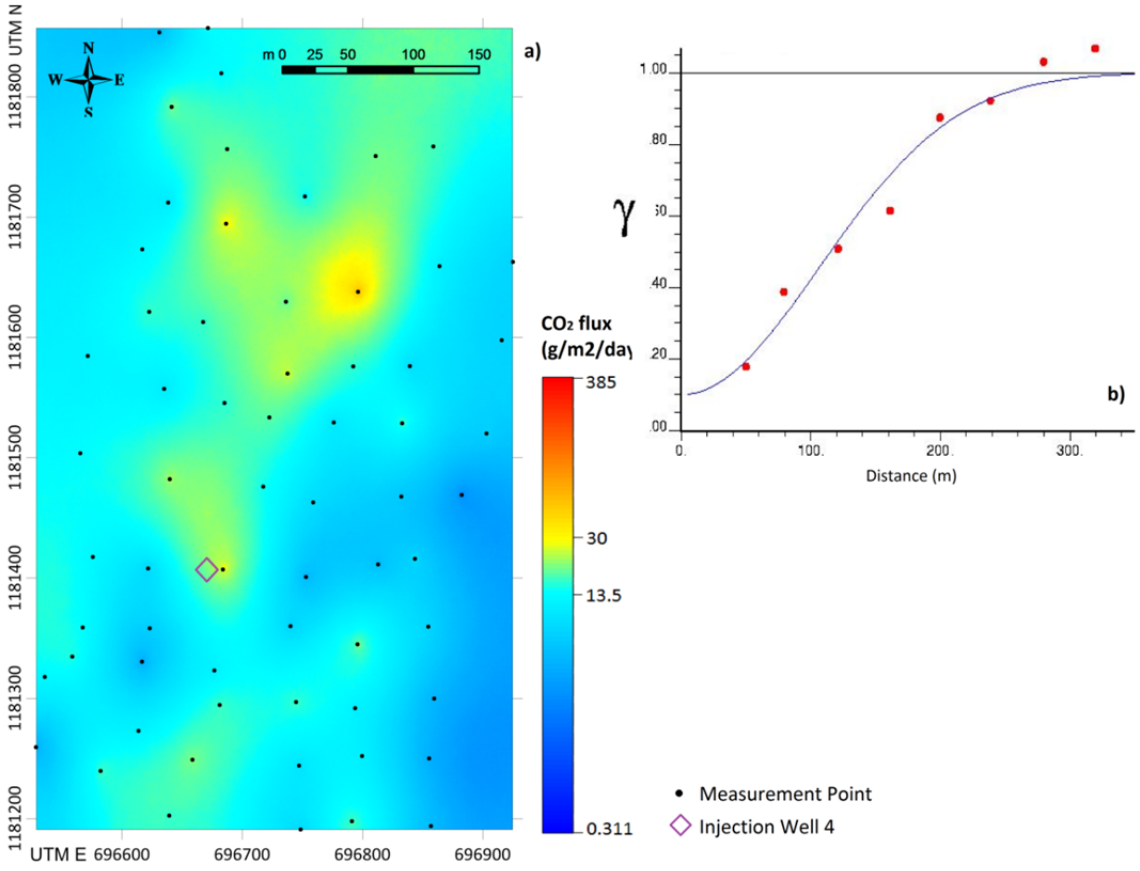

Fig. 15, a) CO_2 flux map of the IW 4 site with measurement locations represented by black dots, logarithmic color scale with significant flux values and b) empirical semi-variogram (red dots) and semi-variogram model (blue line) used for computing CO_2 flux with sGs, horizontal distance of measurement points on the x-axis and ϒ for the variance on the y-axis, where a value of 1 corresponds to a total absence of spatial auto-correlation

5.1.3 "Las Pailas" fumarole area, Rincón de la Vieja

Carbon dioxide efflux at the "Las Pailas" fumarolic area (134 measurements) varied between below the detection limit and 569 g/m^2/day (mean: 33 g/m^2/day, standard deviation: 59 g/m^2/day) where high efflux values were typically measured on altered ground. Inversely, altered grounds frequently did not show high CO_2 efflux, possibly due to sintering of the ground by the hydrothermal activity. The CDP of the LP data set (Fig. 16) shows the presence of two populations of CO_2 efflux, divided at a value of 18 g/m^2/day. The background population represents 64.2 % with a mean of 13 g/m^2/day and the peak population represents 35.8 % of the data with a mean of 70 g/m^2/day.

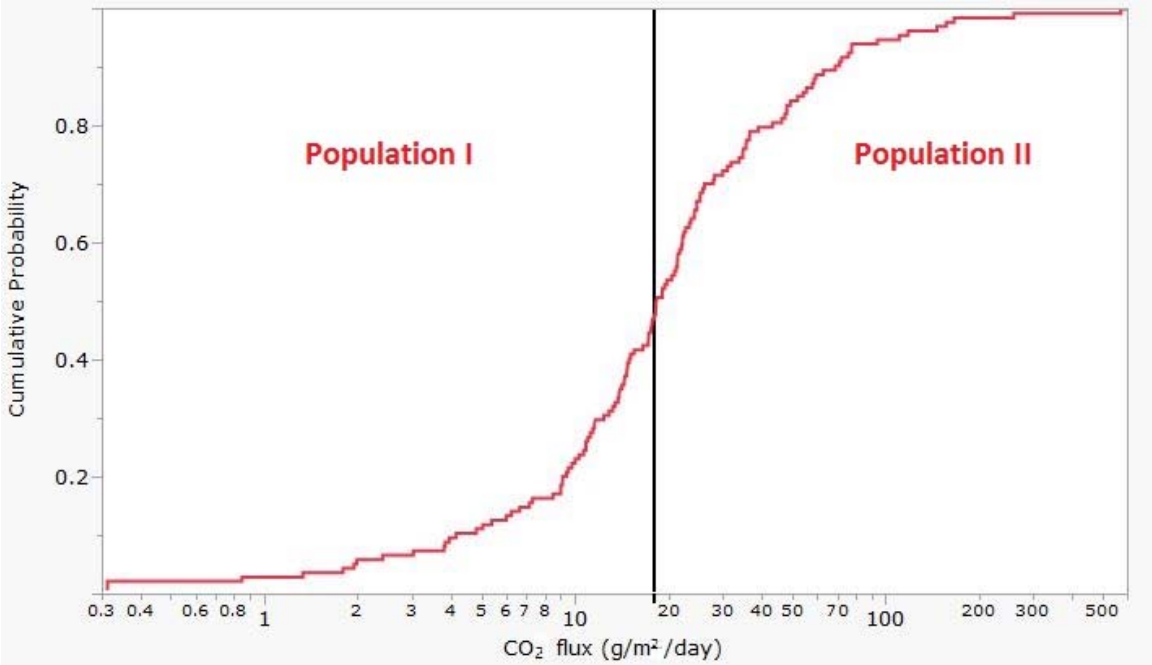

Fig. 16, CDP am of the CO_2 measurements in the LP area with a break point at 18 g/m^2/day, separating background (population I) and peak (population II) flux

A total CO_2 output of 3.3 t/day was calculated for the "Las Pailas" study area using the simulated flux map in Fig. 18a. The total flux ranges from 3.2 to 3.6 t/day (95 % confidence interval) over the area of 0.129 km^2 in 1000 sequential Gaussian simulations, corresponding to a maximum deviation of 7.8 % from the total mean output value. The variogram used for this simulation are presented in Fig. 17a. The empirical variogram shows poor spatial correlation and, therefore, a high nugget effect, causing a strong variability in the model and a less smooth surface of CO_2 flux.

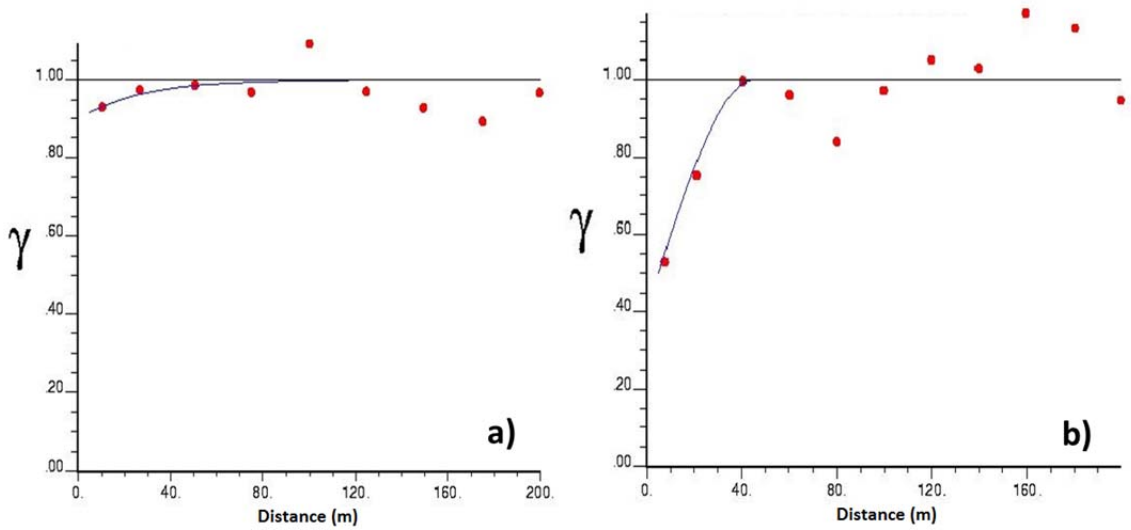

Fig. 17, Empirical (red dots) and modeled (blue line) semi-variograms used for the computation of sGs for a) CO_2 flux and b) soil temperature in the LP area; horizontal distance of measurement points on the x-axis and ϒ for the variance on the y-axis, where a value of 1 corresponds to the total absence of spatial auto-correlation

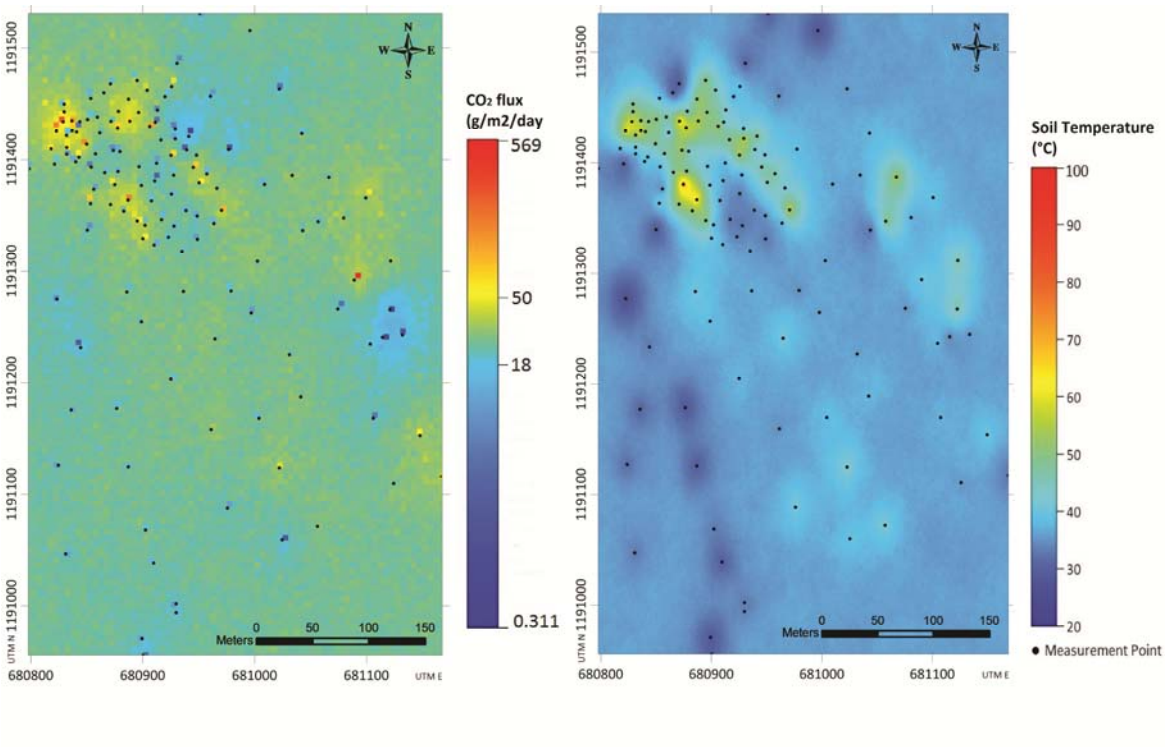

Fig. 18, a) CO_2 flux map of the LP area with measurement locations represented by black dots, logarithmic color scale with significant flux values and b) soil temperature map of the LP area

Soil temperatures in the LP area varied between 23.5 and 98 °C with a mean of 41.3 °C. The empirical variogram of the soil temperature measurements has less variability compared to the variogram of the CO_2 flux from the same area (Fig. 17b), consequently a more detailed map of the soil temperature could be produced for the soil temperature (Fig. 18b). Visual comparison of the soil temperature and CO_2 flux in this area suggests a weak correlation between the two variables (Fig. 19).

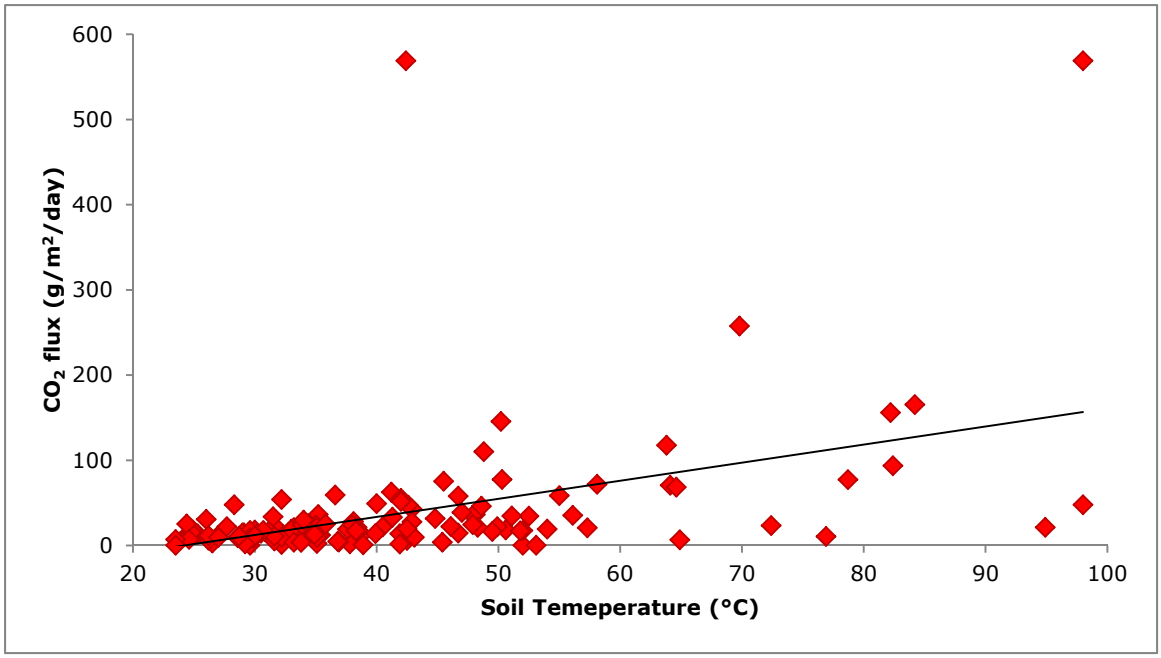

Fig. 19, Positive linear correlation (black line) of CO_2 flux and soil temperature in the LP study area

The LP area shows a positive correlation of CO_2 flux and soil temperature, when visually comparing the two maps and plotted against each other (Fig. 19). The correlation is of rather linear shape and very flat, showing this phenomenon of very low flux in hot altered soil.

In the field it is obvious that high flux is concentrated in surface features (altered soil visible as white patches) and even there this is not always the case. Elevated soil CO_2 flux does not deviate from clusters of altered grounds and even very low flux can be observed around them.

Table 5, Results of soil gas surveys of the three study areas

	Las Hornillas	**Injection Well 4**	**Las Pailas**
Area (km^2)	1.99	0.172	0.129
Max soil temperature (°C)	97.7	33	98
Max CO_2 flux ($g/m^2/day$)	11004	386	569
Mean CO_2 flux ($g/m^2/day$)	253	22	33
Total CO_2 flux (t/day)	**133**	**2.2**	**3.3**
Heat output (MW)	32.4	-	-

5.2 Gas geochemistry

Twelve gas samples in total have been taken from boiling pools and bubbling emissions in the Guanacaste volcanic region in January 2015. Five on the south flank of Rincón de la Vieja, four on the SW side of Miravalles and three at Tenorio (one from the north side and two from the south side of the volcano). 34 samples from older studies (Gherardi et al., 2002; Giggenbach and Soto, 1992; Tassi, unpublished data 1999-2005) were included into the database of gas samples of the Guanacaste region for comparative purposes. These older samples were collected from fumaroles, steam heated pools and wells between 1984 and 2005.

Major and minor constituents of recent and previously analyzed gas samples are reported in Tables 6, 7 and 8 in mmol/mol, with a measurement error of 5 %. In gas discharges on all three volcanoes no HF, HCl or SO_2 concentration has been detected above the detection limit of 0.01 µm/mol. Sampled gases are mainly composed by CO_2 (up to 996 mmol/mol), closely followed by H_2O (up to 995.07 mmol/mol) and the less abundant main species H_2S, N_2, and H_2 (maxima of 35.2, 41.93, 6.33 mmol/mol, respectively). CH_4, Ar and O_2 range up to 1.775, 0.753 and 5.62 mmol/mol, respectively, where Ar and O_2 are more abundant than CH_4 at Rincón, which in turn is more abundant at Miravalles and Tenorio. O_2 concentration varies strongly between different surface features and the volcanoes. Ne, He and CO are present as trace compounds with a maximum concentration of 0.000631, 0.013 and 0.058 mmol/mol, respectively.

Seven different light hydrocarbons (VOCs) were analyzed in the samples, with benzene as the most abundant (max. 78.46 mmol/mol), then ethane, propene, n-butane, propane, butene in descending order and iso-butene with the lowest maximum concentration of 1.9 mmol/mol.

$\delta^{13}C_{CO2}$ values range from -0.63 to -5.44, relative to the PDB standard and He-isotopic values R/Ra vary between 3.24 at Miravalles and 7.1 at Tenorio.

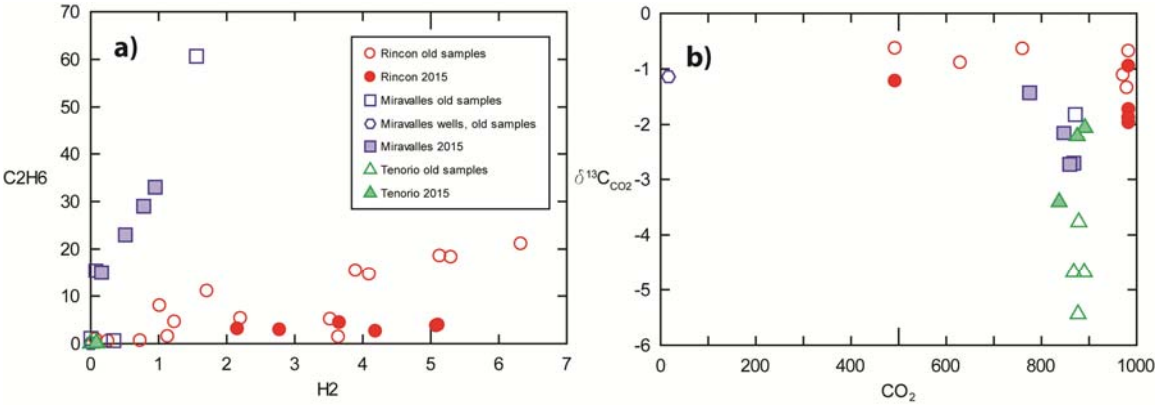

Fig. 20, a) H_2-C_2H_6 and b) CO_2-$\delta^{13}C_{CO2}$ diagrams for Rincón de la Vieja (red), Miravalles (blue) and Tenorio (green) volcanoes; filled symbols represent samples from this study in 2015, empty symbols represent samples from Giggenbach & Soto (1992), Gherardi et al. (2002) and Tassi et al. (2005), and unpublished data of samples collected by F. Tassi (Università degli Studi di Firenze)

Rincón de la Vieja differs in several ways from the other two volcanoes of the Guanacaste region:

Fairly high and variable H_2 contents are typical (Fig. 20a and Fig. 21b), which are three orders of magnitude more than at Tenorio and an order of magnitude more than at Miravalles. Furthermore, Rincón shows comparatively low CH_4 (Fig. 21a and b) and low C_2H_6 contents (Fig. 20a), compared to Miravalles, while Tenorio shows almost no C_2H_6. Higher $\delta^{13}C_{CO2}$ values and less uniform CO_2 values (Fig. 20b) distinguish Rincón from Miravalles and Tenorio.

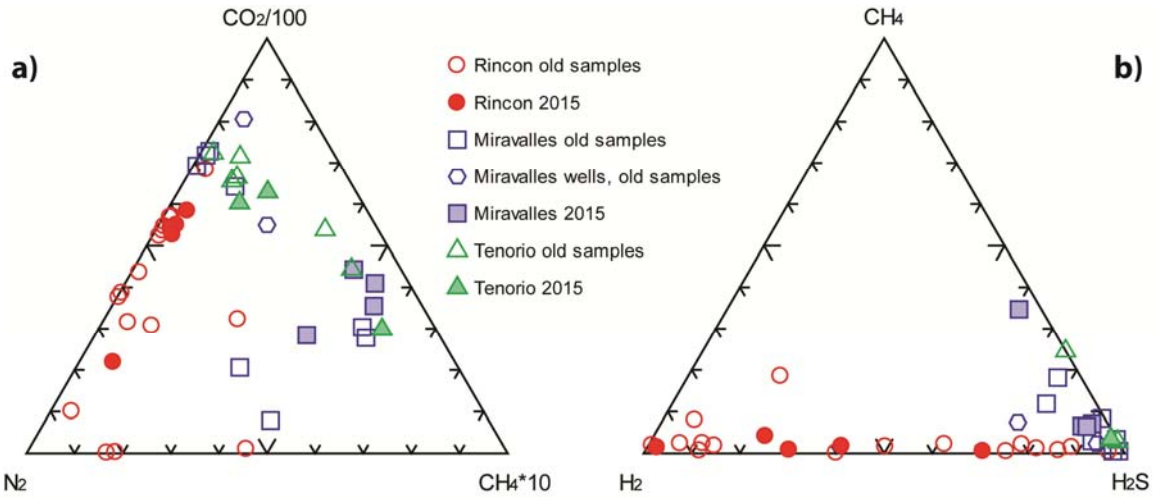

Fig. 21, a) N_2-CO_2-CH_4 and b) H2-CH_4-H_2S ternary diagrams for Rincón de la Vieja (red), Miravalles (blue) and Tenorio (green) volcanoes. Filled symbols represent samples from this study in 2015, empty symbols represent samples from Giggenbach & Soto (1992), Gherardi et al. (2002) and Tassi et al. (2005), and unpublished data of samples collected by F. Tassi (Università degli Studi di Firenze)

Table 6, Chemical composition (in mmol/mol) and helium (expressed as R/Ra) and carbon (expressed as $\delta^{13}C_{CO2}$) isotopic ratios of sampled gases in the Guanacaste volcanic region in January 2015 (red = Rincón, blue =Miravalles, green = Tenorio)

Sample	T°C	CO_2	H_2S	H_2O	N_2	CH_4	Ar	O_2	Ne	H_2	He	CO
Laguna Rincon	92	983.53	1.50	156.00	7.40	0.066	0.130	0.230	0.00011	2.160	0.003900	0.000910
Pailas de Barro	60	983.37	1.80	221.00	7.80	0.053	0.170	0.390	0.00012	4.190	0.003700	0.001100
Pailas de Agua	95	983.57	0.11	117.00	8.10	0.076	0.190	0.280	0.00013	5.110	0.004500	0.001600
Borinquen	94	983.47	8.80	154.00	6.30	0.071	0.160	0.310	0.00008	3.660	0.002100	0.001200
Rincon fumincco	94	492.77	0.89	130.00	16.00	0.160	0.420	0.890	0.00021	2.780	0.003900	0.000900
Las Hornillas 1 2015	97	867.80	14.00	115.00	1.50	1.100	0.014	0.026	0.00001	0.510	0.000350	0.051000
Las Hornillas 2 2015	97	859.33	12.00	125.00	1.90	0.890	0.011	0.031	0.00001	0.780	0.000260	0.058000
Las Hornillas 3 2015	60	847.24	18.00	130.00	2.40	1.300	0.017	0.056	0.00001	0.950	0.000490	0.035000
Guayacan	97	775.00	2.10	213.00	7.50	1.200	0.089	0.150	0.00006	0.160	0.000390	0.011000
Borbollones	30	837.00	1.89	156.00	3.15	1.660	0.061	0.078	0.00004	0.000	0.000230	0.000550
Alto masís 1	81	891.00	6.23	98.00	3.78	0.210	0.035	0.033	0.00002	0.091	0.000510	0.002800
Alto masís 2	68	875.00	7.11	115.00	2.56	0.260	0.025	0.025	0.00002	0.085	0.000470	0.003600

Sample	$d^{13}C$	R/Ra	C_3H_6	i-C_4H_{10}	n-C_4H_{10}	i-C_4H_8	C_6H_6
Laguna Rincon	-1.73	-	0.110	0.160	0.110	0.440	1.300
Pailas de Barro	-0.95	-	0.230	0.078	0.055	0.120	1.100
Pailas de Agua	-1.97	-	0.190	0.110	0.084	0.130	1.500
Borinquen	-1.88	-	0.220	0.550	0.210	0.260	1.900
Rincon fumincco	-1.22	-	0.170	0.140	0.077	0.170	1.100
Las Hornillas 1 2015	-2.71	-	0.085	0.690	1.300	0.510	11.000
Las Hornillas 2 2015	-2.73	-	0.096	0.710	1.500	0.590	15.000
Las Hornillas 3 2015	-2.16	-	0.110	0.850	1.700	0.570	9.300
Guayacan	-1.43	-	0.023	0.510	0.850	0.160	1.500
Borbollones	-3.41	-	0.001	0.002	0.003	0.011	0.071
Alto masís 1	-2.06	7.100	0.003	0.002	0.002	0.019	0.160
Alto masís 2	-2.22	-	0.003	0.001	0.002	0.014	0.170

Table 7, Major and minor constituents (in mmol/mol) and helium (expressed as R/Ra) and carbon (expressed as $\delta^{13}C_{CO2}$) isotopic ratios of the Guanacaste volcanoes (red = Rincón, blue =Miravalles, green = Tenorio) sampled prior to 2015

Sample	T°C	CO_2	H_2S	H_2O	N_2	CH_4	Ar	O_2	Ne	H_2	He	CO	$d^{13}C$	R/Ra
Borinquen BQ*	96	10.0	35.20	-	27.00	0.610	0.360	-	0.00056	4.100	0.003000	-	-	-
Pailas LM*	98	3.70	24.30	-	18.00	0.360	0.250	2.300	0.00035	5.300	0.013000	-	-	-
Pailas vent LV*	98	9.70	14.90	-	5.00	0.420	0.030	0.020	0.00006	3.900	0.003300	-	-	-
Pailas de agua 1***	92.6	983.5	0.08	7.95	7.10	0.030	0.159	-	0.00013	1.135	0.001428	0.000550	-	-
Pailas de Agua 2***	96	983.3	0.13	6.81	8.24	0.029	0.187	0.192	0.00016	1.018	0.002205	0.001766	-	-
Lago Caliente 1***	94	983.5	0.02	8.00	7.93	0.024	0.146	-	0.00014	0.256	0.001805	0.000776	-	-
Lago Caliente 2***	85.5	983.4	0.01	7.88	7.22	0.025	0.133	0.014	0.00012	1.235	0.002312	0.000727	-0.68	-
Pailas de Barro ***	89	492.7	6.39	450.5	41.94	0.216	0.753	1.029	0.00063	6.328	0.002118	0.002775	-0.63	4.12
Pailas do Volc***	98.5	760.8	0.68	225.7	9.41	0.656	0.136	0.315	0.00012	2.205	0.001417	0.001598	-0.64	4.00
Borinquen 1 ***	75	979.8	0.28	5.50	12.28	0.038	0.262	0.005	0.00023	1.713	0.002813	-	-1.34	-
Borinquen 2***	96	979.9	0.45	7.24	8.66	0.028	0.163	0.002	0.00014	3.526	0.001376	0.001166	-	-
Borinquen 3***	96	971.9	2.41	8.61	16.01	0.010	0.323	0.620	0.00018	0.077	0.000473	0.005289	-1.11	-
Borinqu. Barro 1***	95	629.8	15.82	336.1	12.60	0.107	0.244	0.010	0.00021	5.136	0.001792	0.008458	-0.89	3.78
Borinqu. Barro 2***	96	736.8	2.43	245.2	11.59	0.009	0.226	-	0.00014	3.646	0.000199	0.010852	-	-
Borinqu. 1 '05***	94.3	926.7	4.66	63.43	3.86	0.042	0.091	-	0.00005	0.730	0.000549	0.001114	-	-
Borinqu. B. 2	92.3	904.0	8.59	63.77	17.23	0.314	0.398	0.560	0.00024	5.084	0.002642	0.007926	-	-
HN1 Las Hornillas**	64	996.0	0.04	-	4.31	0.011	0.108	0.370	-	0.000	0.000400	-	-	-
HN2 Las Hornillas**	82	992.0	3.88	-	3.69	0.020	0.090	0.319	-	0.089	0.001100	-	-	-
HN3 Las Hornillas**	76	990.0	5.31	-	3.77	0.173	0.102	0.465	-	0.310	0.001100	-	-	-
HN4 Las Hornillas**	75	986.0	9.14	-	5.22	0.000	0.137	0.603	-	0.000	0.000700	-	-	-
HN5 Las Hornillas**	72	992.0	4.04	-	3.47	0.023	0.026	0.133	-	0.039	0.001000	-	-	-
Hornillas pequ. HM*	96	52.0	8.80	-	3.00	0.310	0.030	0.770	0.00004	0.004	0.00250	-	-	-
Las Hornillas 1	58	871.2	11.68	108.6	4.87	1.775	0.109	0.020	0.00009	1.557	0.002071	0.002179	-1.82	3.24
Las Hornillas 2	71	726.1	13.10	242.7	15.98	1.200	0.264	0.477	0.00021	0.076	0.000761	0.000631	-	-
Las Hornillas 3	56	697.3	5.34	291.5	3.46	1.256	0.064	0.570	0.00004	0.339	0.001952	0.000074	-	-
Pozzo 11	98	16.66	0.04	983.2	0.03	0.001	0.000	0.008	0.00000	0.002	0.000006	0.000001	-1.14	-
Pozzo 63	98	4.88	0.02	995.0	0.02	0.002	0.000	0.000	0.00000	0.005	0.000009	0.000002	-	-
Tierras Morenas	91	380.0	1.60	-	11.00	-	0.280	5.620	0.00015	-	0.002600	-		-
Hervideros	94	910.3	2.87	83.24	2.11	0.932	0.048	0.454	0.00004	0.001	0.000095	0.000694	-	-
Poza Celeste	21	878.4	0.31	118.1	1.80	0.575	0.042	0.656	0.00004	0.000	0.000040	-	-3.77	-
Termal Caliente	80	879.7	3.62	112.6	3.29	0.133	0.064	0.505	0.00003	0.000	-	0.003950	-	-
Termal Fria	21	867.8	2.55	126.2	2.41	0.106	0.060	0.695	0.00005	0.000	0.000026	0.000371	-4.68	-
Bambù	36	876.9	1.14	118.5	3.03	0.139	0.071	0.105	0.00005	0.000	0.000104	-	-5.44	-
Termal Rio Celeste	27.5	889.7	1.15	105.5	3.07	0.033	0.048	0.410	0.00003	0.001	0.000110	0.000177	-4.68	-

* Samples from (Giggenbach and Soto, 1992), ** Samples from (Gherardi et al., 2002), *** Samples from (Tassi et al., 2005), unmarked samples are unpublished data collected by F. Tassi

Table 8, Light hydrocarbon concentrations (in mmol/mol) of the Guanacaste volcanoes (red = Rincón, blue =Miravalles, green = Tenorio) sampled prior to 2015

Sample	C_2H_6	C_3H_8	C_3H_6	i-C_4H_{10}	n-C_4H_{10}	i-C_4H_8	C_6H_6
Borinquen BQ*	14.600	2.800	0.100	0.200	0.800	-	17.700
Pailas LM*	18.300	4.100	0.600	0.200	1.000	-	17.000
Pailas vent LV*	15.400	3.100	-	0.200	0.800	-	3.200
Pailas de agua 1***	1.483	0.025	0.573	0.057	0.103	0.362	2.248
Pailas de Agua 2***	7.953	0.029	0.703	0.043	0.172	0.180	2.689
Lago Caliente 1***	0.503	0.019	0.257	0.113	0.304	0.121	1.664
Lago Caliente 2***	4.574	0.050	0.752	0.040	0.180	0.078	1.494
Pailas de Barro ***	21.099	0.511	4.851	0.689	2.243	4.617	22.063
Pailas do Volc***	5.292	0.148	1.069	0.190	0.305	1.141	4.446
Borinquen 1 ***	11.042	0.217	1.551	0.083	0.492	0.155	5.121
Borinquen 2***	5.123	0.143	2.499	0.132	2.005	0.783	-
Borinquen 3***	0.897	-	0.341	0.029	0.046	0.071	0.310
Borinquen Barro 1***	18.527	0.979	17.668	1.902	16.093	8.725	-
Borinquen Barro 2***	1.381	0.101	0.731	0.035	0.133	0.191	8.505
Borinquen 1 2005***	0.604	0.092	0.005	0.008	0.016	0.048	0.304
Borinquen Barro 2 2005***	3.707	0.579	0.010	0.041	0.108	0.030	1.685
HN1 Las Hornillas**	-	-	-	-	-	-	-
HN2 Las Hornillas**	-	-	-	-	-	-	-
HN3 Las Hornillas**	-	-	-	-	-	-	-
HN4 Las Hornillas**	-	-	-	-	-	-	-
HN5 Las Hornillas**	-	-	-	-	-	-	-
Hornillas pequenas HM*	1.100	0.200	0.001	-	0.050	-	0.800
Las Hornillas 1	60.638	11.384	0.222	0.546	1.109	-	78.461
Las Hornillas 2	15.399	3.397	0.054	0.124	0.776	0.353	4.658
Las Hornillas 3	0.612	2.156	0.046	-	0.030	0.013	0.255
Pozzo 11	0.024	0.007	0.001	0.000	0.002	0.001	0.004
Pozzo 63	0.022	0.007	0.000	0.000	0.001	0.001	0.003
Tierras Morenas TM*	4.800	0.500	0.022	-	0.100	-	5.400
Hervideros	0.094	0.036	0.003	0.004	0.010	0.040	0.085
Poza Celeste	0.049	0.025	-	0.002	0.008	0.009	0.003
Termal Caliente	0.066		-	-	0.003	0.008	1.613
Termal Fria	0.020	0.005	-	0.002	0.002	0.004	0.036
Bambù	0.069	0.015	-	-	0.003	0.006	0.001
Termal Rio Celeste	0.019		-	-	-	0.058	2.481

* Samples from (Giggenbach and Soto, 1992), ** Samples from (Gherardi et al., 2002), *** Samples from (Tassi et al., 2005), unmarked samples are unpublished data collected by F. Tassi (Università degli Studi di Firenze)

6. Discussion

6.1 Diffuse soil gas flux

6.1.1 "Las Hornillas" area, Miravalles power plant

Distribution of soil flux and soil temperatures and structural control

Peak CO_2 flux is obviously concentrated in areas of ground alteration and fumarolic fields. Outside these visible surface expressions of the hydrothermal system, CO_2 flux drops rapidly to background or "mixed" flux values. Mixed flux values are apparently not enough for stressing vegetation, since only stressed vegetation was observed, where high CO_2 soil flux and elevated soil temperatures were measured. Very low flux (around the LOD or below) was observed in the very NE of the LH study area, which is an abandoned quarry (Fig. 8, Zone B). Since a minimum of about 75 % of the quarry is vegetation and soil free, there is almost no CO_2 flux (no biogenic CO_2 input) and the existing measured CO_2 is possibly due to air contamination. The bed rock is hard and massive basalt/basaltic andesite with little porosity and no visible fractures in this area, leaving no space for diffuse soil gas flux. This shows the contrast between vegetated and non-vegetated areas outside the DDSs, indicating that the background CO_2 flux is obviously derived from the decomposition of biogenic material.

The Zone A in Fig. 8, between the two fumarolic fields, is a large zone of low to mixed flux with a very wide spacing of measurement locations. This wide spacing is suspected to cause incorrect interpolation of higher flux values than the actual measurements around (dark blue patches). Close to these low flux measurements, the program simulates the flux correctly as low, but after 30 - 50 m distance, suddenly higher flux is simulated. This is probably due to the shape of the variogram model, where the strongest spatial auto-correlation is until about 50 m distance. After this strong decrease of spatial auto-correlation, the model takes the low-flux neighbors with a similar weight into account than the higher-flux points further away. Therefore the flux is simulated higher than logically expected. This error leads presumably to an over-estimation of the local CO_2 flux and, therefore, to an over-estimation of the total CO_2 output of this study area.

Miravalles volcano is influenced by several regional lineaments and faults. The Las Hornillas study area and its surface expressions of the deep hydrothermal system lie along such a fault (RL 5 in Fig. 3, section 2/Geological Setting; and Melián et al. 2004, Fig. 2), typical for DDSs. The fault is NE-SW orientated and crosses the whole volcanic complex, including the old Guayabo caldera. Faults create a zone of higher permeability, enabling deep fluids to rise to the surface, creating altered zones in some cases. Therefore, it is assumed that there is a direct link between tectonic and degassing structures.

Diffuse carbon dioxide flux in volcanic regions is often correlated with elevated soil temperatures (e.g. Bloomberg et al. 2014; Werner et al. 2008). In the LH area a positive logarithmic relationship between CO_2 flux and soil temperature was observed (Fig. 11). This indicates that hot steam from the deep hydrothermal reservoir and CO_2 travel along the same pathways to the surface. It also gives additional support for the assumptions that the flux in the previously mentioned Zone A, between the two fumarolic fields, is over-estimated, since no elevated soil temperatures were observed in this area. The concentration of CO_2 flux and elevated soil temperature in and around surface features of the hydrothermal systems could indicate that the transport of heat and gas is dominated by advective processes rather than diffusion, which is possibly the main transport process for CO_2 from biogenic sources (Chiodini et al., 2001).

Comparison to previous study at Miravalles

The calculation of CO_2 output in the selected LH and IW 4 areas is an attempt for more detailed knowledge about diffuse degassing distribution and behavior at Miravalles. The only previous study of diffuse degassing at Miravalles by Melián et al. (2004) was focused on the calculation of a total CO_2 output by the Miravalles volcano with significantly less detail. They conducted 244 measurements over an area of 65 km^2, whereas in this study the calculations for the two study areas are based on 500 measurement points in roughly 2 km^2. Here, only areas of anomalous flux and surface expressions of hydrothermal fluids were investigated, since it can be assumed that magmatic CO_2 emissions of quiescent volcanoes are mainly focused in DDSs, shown by previous studies (Chiodini et al., 2001, 1998; Gerlach et al., 2001; Hernández et al., 1998). These are located above fracture zones which act as pathways for hydrothermal fluids. It is likely that the edifice of Miravalles volcano is

strongly impermeable for diffuse transport from the deep reservoir, suggested by the very low flux values in the quarry region (Fig. 8, Zone B). In this part of the LH study area, vegetation is stripped away, only leaving the impermeable bedrock consisting of lava flows and lahar deposits, where the transport of magmatic CO_2 is dominated by fracture zones.

This study provides a clearly more detailed estimation of diffuse carbon dioxide flux from the soil with a more systematic sampling approach and likely smaller error, compared to the work of Melián et al. (2004), who probably strongly overestimated the total output of magmatic CO_2 by Miravalles volcano. The interpolation of a small amount of data in combination with unequal spacing and the lack of detail in high-flux zones can lead to an inaccurate estimate of the total CO_2 output. Biogenic CO_2 represents a large part of diffuse soil degassing at Miravalles, which interferes with the estimate of magmatic CO_2 output. The combination of this study with further detailed studies of the summit area and other high flux areas indicated by Melián et al. (2004) in the N and SE of the volcanic complex can lead to a more detailed estimation of the volcano's output in carbon dioxide. Detailed measurements of the LH area can be used for chemical monitoring of the volcano, since it is an easily accessible area and, therefore, changes in its degassing behavior can be easily detected. This is also of benefit for the geothermal power plant, where its use and safety issues rely directly on the volcano's activity.

Heat flow estimation

Heat flow was estimated in the LH area using $[H_2O]$:$[CO_2]$ mass ratios of gas discharges in two different wells (Pozo 11 and 63) of the geothermal power plant. The estimation of heat flow, extrapolated over the whole geothermally exploited area of 3.8 MW and 13.3 MW is comparatively low to the production design of the power plant, which is about 163 MW. This large discrepancy suggests that the ratio of $[H_2O]$:$[CO_2]$ is not a suitable proxy for heat flow estimations in this area due to several possible reasons: 1) Gas emissions at the deep geothermal wells might not have the same composition as in the high upflow zones, where escaping gases are concentrated and, therefore, it is difficult to compare thei with the gas data of the wells with diffuse degassing in the DDSs. 2) Interaction of uprising gases with the rock and shallow ground water, can reduce the diffuse soil degassing, as well as the CO_2 concentrations in fumaroles and bubbling pools. The shallow water table can be

assumed to be far more extensive due to the large amounts of rainfall in this area, compared to volcanic areas with dryer climate, where this method of heat flow estimation was used. 3) If most of the CO_2 is emitted by surface features (e.g. bubbling hot pools and fumaroles), it would not be included into the calculations, because only diffusely degassed CO_2 was used for the estimation and, therefore, a large part of heat flow would have been missed, explaining the present discrepancy. 4) Additionally, the fact that well 63 has stopped producing in 2003, after one year of use, suggests that higher gas and heat flow can be expected in other areas and that this well is not a suitable location for a representative $[H_2O]$:$[CO_2]$ ratio. It is assumed that the decrease of natural permeability and the formation of sinter around the well, due to lower flashing because of geothermal extraction, could be reasons for this well to have stopped producing (Moya and Yock, 2005). Therefore, it is likely that this well does not represent the original $[H_2O]$:$[CO_2]$ ratio derived from fluids from the deep hydrothermal reservoir. To further investigate the use of this method of heat flow estimation further data on gas compositions from geothermal wells in the power plant area would be needed.

6.1.2 Injection Well 4 site, Miravalles power plant

Carbon dioxide flux around the Injection Well 4 shows generally slightly elevated values compared to background values and anomalous amounts of flux are present. Although, they are not comparable to the fumarolic fields at the LH site. Interestingly, the highest values of CO_2 flux are not directly next to the well or on the well site, but outside, near other groundwater wells. ICE reported problems with the re-injection of waste-fluid produced by the power plant. Therefore, it is most likely that elevated carbon dioxide flux in the soil is artificially induced by the re-injection, rather than due to a natural surface emanation of the deep hydrothermal system. Ground alteration on the injection well site is probably due to escaping gases from the Cl-rich brine or percolation of the waste water itself in shallow levels of the soil.

Anomalous flux was also observed next to the creek along the well site, which additionally showed rising gases in the water. This could indicate that gas is escaping from the injection and is transported through fractures back to the surface. Carbon dioxide emissions at the surface are probably due to short-curcuit circulation of the

injected gas, and are, therefore, showing a leak of this injection well site. Topography and the location of the creek suggest that this depression could be such a fracture zone, explaining problems with the injection at this site and not others, where there is no fracture zone in direct surroundings. Visual evidence of this lateral escape is only observed on and around the well site, where some m^2 of altered ground can be found and a strong H_2S smell is present. Dead animals and bones were found along the creek located in the depression, suggesting that CO_2 is escaping and gathering close to the surface, suffocating creatures near the ground.

6.1.3 "Las Pailas" area, Rincón de la Vieja

Distribution of soil flux

The "Las Pailas" area is composed of several fumarolic fields with hot pools, mud pools, frying pans and fumaroles, generally showing elevated soil flux of CO_2. High flux values were observed around and near these features as expected. Surprisingly, most of the altered ground shows very low flux values (close the background values), unlike in the LH area. This is either due to natural strong concentration of gas flux in the surface features and/or the shift of degassing from the soil to these features due to the self-sealing effect of ground alteration by gradual sinter-precipitation (Facca and Tonani, 1967). Chiodini et al. (2001) suggested that the transporting mechanism for deeply derived hydrothermal CO_2 is rather advection with the rising magmatic gas body, in contrast with biogenically derived CO_2, which rises dominantly by diffusion mechanics. The effect of these two mechanisms could be the reason for this particular distribution of CO_2 flux, which has a strong effect on their spatial auto-correlation. It creates a high variability in the CO_2 flux variogram and thus in the sequential Gaussian simulations. Therefore, high flux zones are more isolated dots rather than distinguished zones, visible in Fig. 18. Simulated values are therefore less reliable, due to the weakness of the variogram model.

The correlation of CO_2 flux and soil temperature (Fig. 19) is a rather flat curve compared to curve for LH, which means rather low CO_2 flux at high temperature. This again supports the idea of self-sealing ground-alteration where only heat is transported by conduction and no diffuse transport of gases is possible.

Comparison of diffuse degassing behavior of Rincón de la Vieja and Miravalles

In comparison to the Las Hornillas zone, the Las Pailas study area has about 65 % less of CO_2 discharge from diffuse soil degassing, if both areas were of similar extent; even though the LH area mainly consists of unaltered ground with low background values far from the fumarolic fields. Less diffuse degassing on the flanks/base of the active volcano Rincón de la Vieja compared to the dormant Miravalles could indicate a different degassing behavior if the hypothesis of a common hydrothermal reservoir (Giggenbach and Soto, 1992) applies. Although they both show secondary degassing features on the flanks/bases, generally lower flux values were observed at Rincón de la Vieja, even in strongly altered soils. This could be either due to stronger concentration in the surface features (fumaroles and steam heated pools) than through the soil on this volcano or generally more focused degassing around the Active Crater area. Weaker soil degassing has been attributed to activity states with stronger plume-degassing (Notsu et al., 2006). Since Rincón de la Vieja was historically and recently very active, it is possible that the active magma plumbing system towards its Active Crater facilitates the transport of gas to the surface, compared to the degassing paths towards the flanks. Miravalles on the other hand has not recently been active and does not show evident emissions of CO_2 on the summit (summit crater is fully vegetated, which indicates no lethal amounts of CO_2 for plants), which indicates that at this dormant volcano, gas escapes mainly through the flanks. Since it is unclear if these two volcanoes have a common hydrothermal reservoir or not, these differences in degassing behavior could also be attributed to the possible existence of two separate hydrothermal systems with completely different physical and chemical conditions.

Possibilities for monitoring

Similarly to Miravalles, this study of diffuse degassing in the LP zone can be utilized for geochemical monitoring purposes at Rincón de la Vieja volcano. Certainly, the summit region is the center of activity and therefore the most accurate location for geochemical monitoring and, like Tassi et al. (2005) indicated, an important part of the magmatic gases escaping from the volcano outside the summit crater region is strongly interacting with shallow groundwaters. Nevertheless, degassing behavior and intensity can be monitored by repeated measurements of diffuse soil CO_2 and a

long-term evolution of the system can be investigated in a more easily accessible area, since the summit region of Rincón de la Vieja is very sparsely accessibly throughout the year.

6.2 Gas geochemistry

Rincón de la Vieja, Miravalles and Tenorio are spatially very close, aligned on the Central Volcanic Belt and belong to a one of Costa Rica's active volcanic regions. General similarities in magmatic compositions (Chiesa et al., 1994) have been determined and relatively uniform water discharges were found by Giggenbach & Soto in 1992, who suggested a common geothermal reservoir beneath the Guanacaste volcanic region.

Abundances of several species, like H_2O, CO_2, H_2S, CO and the general absence of SO_2, HF or HCl are common to all three volcanoes in the region and do not allow a distinction among them. Nevertheless, certain elements show more or less distinct trends that allow a distinction of the different volcanoes.

Origin of volcanic gases

A remarkably high R/Ra ratio of 7.1 was measured in this study at Tenorio. Previous measurements by Giggenbach and Soto (1992) also showed R/Ra ratios up to 7.2 in sampled gases at Miravalles, which suggests a more primitive source and therefore stronger mantle signature (Sigurdsson et al., 1999) at these two volcanoes, which are both dormant. On the other hand, at Rincón de la Vieja ratios vary between 3.78 and 4.12. This suggests that Tenorio and Miravalles are not in the periphery of major upflow zones of magmatic fluids as was suggested for Tenorio by Giggenbach and Soto (1992), but are still fed by fluids derived from relatively primitive magma.

The He-N_2-Ar ternary diagram (Fig. 22a) is widely used for the derivation of origin and the determination of atmospheric influence of volcanic gases (Garofalo et al., 2007; Giggenbach and Soto, 1992; Sigurdsson et al., 1999; Tassi et al., 2005). For the Guanacaste region a strong influence by air and air saturated water is visible, a hint for strong hydrothermal activity. Nevertheless, there is a trend towards the convergent plate boundary endmember to observe, which is in accordance with the tectonic setting.

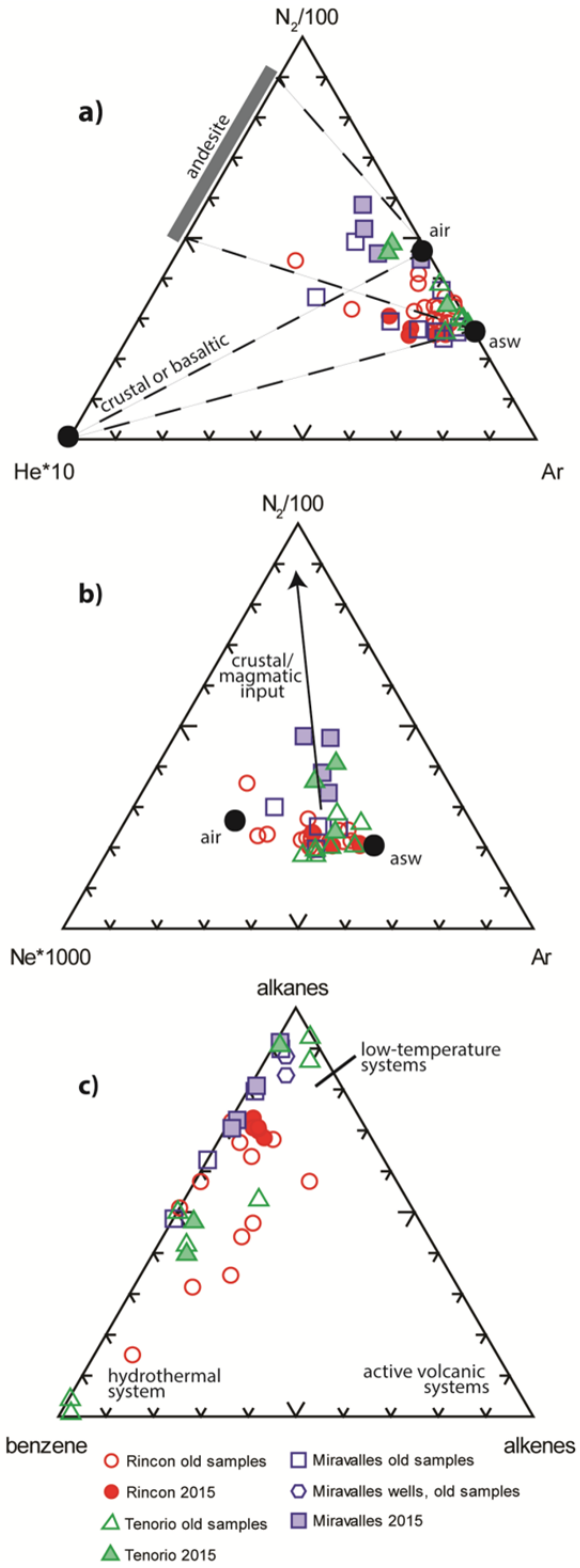

Fig. 22, a) He-N_2-Ar ternary plot showing input from andesite, crust, basalt, air and air saturated water on the gas emissions b) Ne-N_2-Ar ternary plot indicating crustal or magmatic input in Miravalles and Tenorio samples (asw = air saturated water) and c) ternary diagram of light hydrocarbons and their origin

A slightly higher abundance of N2 is observed at Miravalles and Tenorio in Fig. 22b compared to Rincón de la Vieja. This suggests either magmatic or crustal input into the hydrothermal system. For the distinction of these two components, further nitrogen and helium isotopic analysis would be beneficial. Abundance of N2 in hydrothermal gases is typical for gases from an andesitic system as indicated in Fig. 22a.

Carbon isotopic compositions between -5.44 and -0.63 are typical for subduction related volcanic gas emissions (Sigurdsson et al., 1999), showing mantle-derived carbon, contaminated by carbon-bearing sediments. These sediments vary around the PDB-standard (defined by the Pee Dee Belemnite, representing typical carbon-bearing sediments), influencing the $\delta^{13}C_{CO2}$ values towards less negative values. $\delta^{13}C_{CO2}$ values of samples taken from the accumulation chamber have typical values for a volcanic environment with magmatic as well as sedimentary input. Due to the scarcity of data, the usual positive correlation between the two variables could not be observed.

It is noticeable that air-derived species, such as O_2, Ne and Ar are more abundant in gases sampled at Rincón de la Vieja, suggesting air entrainment into the shallow ground interacting with rising fluids, where different amounts of O_2 could indicate different amounts of air contamination at the three volcanoes.

Hydrothermal processes

In general, no HF, HCl or SO_2 were measured in the gas sampled on the flanks/bases of the volcanoes. These acid species are typical for active volcanic systems dominated by high temperatures derived from possible magmatic sources (Vaselli et al., 2006) . The absence of these species suggests that the possible inflow of magmatic fluid is efficiently buffered by hydrothermal reservoirs present in the subsurface of the three volcanoes of the Guanacaste region (Giggenbach and Soto, 1992; Tassi et al., 2005). Interaction with liquid water causes their dissolution, preventing them from reaching the surface (Tassi et al., 2005). This process masks the magmatic input, which would usually be traceable in high-temperature fumarolic emissions. Only at Rincón de la Vieja in the summit crater could these species be detected in the emitted gas (Tassi et al., 2005). In addition, the low contents of H_2S

suggest either the removal of these species through reaction with O_2 in shallow groundwater (Tassi et al., 2005), or the precipitation of sulfides due to gas-rock interaction in depth and around the surface features (Gherardi et al., 2002), the latter being observed in the field.

VOCs

Proportions of light hydrocarbons can be used to distinguish the physical conditions of the source of the sampled gas. Alkenes are produced at high temperatures close to magmatic conditions and most of them are not stable at low temperatures (<300 °C), while alkanes are typical for low-temperature regimes, derived from biogenic degradation and disintegrating alkenes when submitted to lower temperatures. Finally, aromatics such as benzene are usually produced in hydrothermal environments by the interaction of a hot magmatic fluid with CH_4-rich fluids from sediments, present in subduction zones (Capaccioni et al., 2004; Capecchiacci, 2012). In the Guanacaste region concentrations of light hydrocarbons (Fig. 22c) vary between the alkane and benzene end members, indicating the hydrothermal overprint of magmatic gases and a strong influence by low-temperature controlled biogenic degradation, typically expected in tropical regions with heavily vegetated surfaces.

7. Conclusions

Diffuse soil flux of CO_2 at Miravalles and Rincón de la Vieja is concentrated in and around surface expressions of their hydrothermal systems, including zones of altered soil and fumarolic fields. The total output of 135 t/day of CO_2 of the investigated part (~2 km^2) of the geothermal power plant at Miravalles is slightly lower, although comparable, to emissions at other volcanogenic geothermal areas (Bloomberg et al., 2014; Werner and Cardellini, 2006). The measurement of CO_2 flux at Rincón de la Vieja's secondary emissions, Las Pailas (0.129 km^2), resulted in a value of 3.3 t/day, which is low in comparison to similar volcanic areas.

Due to the concentration of CO_2 degassing along surface features and low flux values at a distance to them, it can be assumed that the transport of volcanic gases at Miravalles and Rincón de la Vieja is dominated by the process of advection, while diffusion processes mainly transport biogenic CO_2. Due to the lack of correlation of CO_2 flux and carbon isotopic values, this could not be verified, although a statistical separation of flux populations was successful. Furthermore, the concentrated distribution of CO_2 flux at Miravalles shows the difficulty of detecting the extent of the hydrothermal reservoir at depth, tapped by the geothermal power plant, with the accumulation chamber method. This should be combined with measurements of CO_2 emissions through fumaroles and hot pools, as well as the amount of CO_2 diluted in rivers and streams to obtain a complete estimate of CO_2 emissions by the hydrothermal system(s).

Comparatively low CO_2 flux (maximum of 569 $g/m^2/day$) in DDSs at Rincón de la Vieja, with similar properties compared to the ones at Miravalles (maximum 11,004 $g/m^2/day$), indicates even stronger concentration of gas output through surface features and possibly the active summit region. This shows different degassing behavior of the active Rincón de la Vieja and the dormant Miravalles volcano, if the hypothesis of a common hydrothermal system applies. If this is not the case, these variations could be due to the existence of separate hydrothermal systems for each volcano with completely different chemical and physical conditions.

The application of the fairly new method for the calculation of heat flow, by using diffuse degassing output and the $[H_2O]$:$[CO_2]$ mass ratio of fumaroles or wells, showed that this method is not applicable on Miravalles and no valid assessment of

geothermal potential could be calculated. As mentioned before, a more comprehensive calculation of CO_2 degassing is needed.

This study provides further information to the understanding of the compositional variations of gas emission among the three volcanoes, with the analysis of fumarolic gases. Evidence for strong hydrothermal activity could be detected and several compositional similarities and differences among the volcanoes can be observed. Even though acid species were captured by their hydrothermal system(s) and did not reach the surface, significant concentrations of N_2, H_2 and R/Ra values were determined that suggest general andesitic input into the volcanic systems of the Guanacaste region and the presence of fairly primitive magmatic fluids at Tenorio and Miravalles. This could indicate the possibility of continuing magma recharge, not only for the historically active Rincón de la Vieja, but also for the dormant volcanoes Tenorio and Miravalles, which were previously suggested to lie outside major upflow zones of magmatic fluids.

Future work

This study resulted in the first calculation of CO_2 soil degassing at Rincón de la Vieja and adds further detail to the previous study at Miravalles by Melián et al. (2004). In order to obtain a complete mass balance of CO_2 for the Guanacaste volcanoes, studies of pre-eruptive CO_2 contents in the magma, by the use of melt inclusions in juvenile eruptive materials, should be combined with further investigations of degassing at DDSs, vents and fumaroles, as well as the determination of the amount of diluted CO_2 in rivers and streams, leading to a calculation of total CO_2 output into the atmosphere for the studied volcanoes.

Furthermore, a similarly detailed study of all DDSs at Miravalles should lead to a very detailed calculation of CO_2 output at Miravalles and a comparison to the previous study can be made. This could give information about the necessary level of detail for diffuse degassing studies to improve future measurement strategies.

Finally, this work could serve as a foundation for a geochemical long-term monitoring of the Guanacaste volcanoes. By continuous repetition of soil degassing studies and gas chemistry analyses, especially during volcanic and tectonic periods of unrest, the evolution of these volcanic complexes can be studied, as well as a possible influence of geothermal exploration on volcanic hydrothermal systems.

8. References

Allard, P., Carbonnelle, J., Dajlevic, D., Le Bronec, J., Morel, P., Robe, M.C., Maurenas, J.M., Faivre-Pierret, R., Martin, D., Sabroux, J.C., Zettwoog, P., 1991. Eruptive and diffuse emissions of CO2 from Mount Etna. Nature 351, 387–391.

Alvarado, G.E., Gans, P.B., 2012. Síntesis Geocronológica Del Magmatismo, Metamorfismo Y Metalogenia De Costa Rica, América Central. Rev. Geológica Am. Cent. 46, 7–122.

Arpa, M.C., Hernández, P. a., Padrón, E., Reniva, P., Padilla, G.D., Bariso, E., Melián, G. V., Barrancos, J., Nolasco, D., Calvo, D., Pérez, N.M., Solidum, R.U., 2013. Geochemical evidence of magma intrusion inferred from diffuse CO2 emissions and fumarole plume chemistry: The 2010-2011 volcanic unrest at Taal Volcano, Philippines. Bull. Volcanol. 75, 1–13. doi:10.1007/s00445-013-0747-9

Barquero, R., Taylor, W., 1998. Proyecto Geotérmico Tenorio: Los enjambres sísmicos periodo octubre-noviembre de 1997 y 1998: Informe preliminar.

Baubron, J.C., Allard, P., Toutain, J.P., 1990. Diffuse volcanic emissions of carbon dioxide from Vulcano Island, Italy. Nature 344, 51–53.

Bloomberg, S., Werner, C., Rissmann, C., Mazot, A., Horton, T., D.Gravley, Kennedy, B., Oze, C., 2014. Soil CO2 emissions as a proxy for heat and mass flow assessment, Taupo Volcanic Zone, New Zealand. Geochemistry, Geophys. Geosystems 15, 4885–4904. doi:10.1002/2014GC005327.Received

Brusca, L., Inguaggiato, S., Longo, M., Madonia, P., Maugeri, R., 2004. The 2002-2003 eruption of Stromboli (Italy): Evaluation of the volcanic activity by means of continuous monitoring of soil temperature, CO2 flux, and meteorological parameters. Geochemistry, Geophys. Geosystems 5, 1–14. doi:10.1029/2004GC000732

Capaccioni, B., Taran, Y., Tassi, F., Vaselli, O., Mangani, G., Macias, J.L., 2004. Source conditions and degradation processes of light hydrocarbons in volcanic gases: an example from El Chichón volcano (Chiapas State, Mexico). Chem. Geol. 206, 81–96. doi:10.1016/j.chemgeo.2004.01.011

Capecchiacci, F., 2012. Geochimica dei fluidi vulcanici e idrotermali : Origine delle componenti organiche e loro impatto ambientale.

Cardellini, C., Chiodini, G., Frondini, F., 2003a. Application of stochastic simulation to Co2 flux from soil: Mapping and quantification of gas release. J. Geophys. Res. 108, 1–13. doi:10.1029/2002JB002165

Cardellini, C., Chiodini, G., Frondini, F., Granieri, D., Lewicki, J., Peruzzi, L., 2003b. Accumulation chamber measurements of methane fluxes: Application to volcanic-geothermal areas and landfills. Appl. Geochemistry 18, 45–54. doi:10.1016/S0883-2927(02)00091-4

Cerling, T.E., Solomon, D.K., Quade, J., Bowman, J.R., 1991. On the isotopic composition of carbon in soil carbon dioxide. Geochim. Cosmochim. Acta 55, 3403–3405.

Chiesa, S., Alvarado, G.E., Pecchio, M., Corella, M., Zanchi, A., 1994. Contribution to petrological and stratigraphical understanding of the Cordillera de Guanacaste lava flows, Costa Rica. Rev. Geol. América Cent.

Chiesa, S., Civelli, G., Gillot, P.-Y., Mora, a, Alvarado, G.E., 1992. Rocas piroclasticas asociadas con la formacion del la Caldera de Guayabo. Cordillera de Guanacaste, Costa Rica. Rev. Geol. América Cent.

Chiodini, G., Caliro, S., Cardellini, C., Avino, R., Granieri, D., Schmidt, A., 2008. Carbon isotopic composition of soil CO2 efflux, a powerful method to discriminate different sources feeding soil CO2 degassing in volcanic-hydrothermal areas. Earth Planet. Sci. Lett. 274, 372–379. doi:10.1016/j.epsl.2008.07.051

Chiodini, G., Cioni, R., Guidi, M., Raco, B., Marini, L., 1998. Soil CO2 flux measurements in volcanic and geothermal areas. Appl. Geochemistry 13, 543–552. doi:10.1016/S0883-2927(97)00076-0

Chiodini, G., Frondini, F., Cardellini, C., Granieri, D., Marini, L., Ventura, G., 2001. CO2 degassing and energy release at Solfatara volcano, Campi Flegrei, Italy. J. Geophys. Res. 106, 16,213–16,221.

Chiodini, G., Granieri, D., Avino, R., Caliro, S., Costa, a., Werner, C., 2005. Carbon dioxide diffuse degassing and estimation of heat release from volcanic and hydrothermal systems. J. Geophys. Res. B Solid Earth 110, 1–17. doi:10.1029/2004JB003542

Croghan, C.W., Egeghy, P.P., 2003. Methods of Dealing with Values Below the Limit of Detection using SAS.

Deutsch, C.V., Journel, A.G., 1998. GSLIB: Geostatistical software library and user's guide, Oxford University Press.

Facca, G., Tonani, F., 1967. The self-sealing geothermal field. Bull. Volcanol. 30, 271–273. doi:10.1007/BF02597674

Faure, G., Mensing, T.M., 2005. Isotopes: Principles and Applications, John Wiley & Sons Inc.

Fridriksson, T., Kristjánsson, B.R., Ármannsson, H., Margrétardóttir, E., Ólafsdóttir, S., Chiodini, G., 2006. CO2 emissions and heat flow through soil, fumaroles, and steam heated mud pools at the Reykjanes geothermal area, SW Iceland. Appl. Geochemistry 21, 1551–1569. doi:10.1016/j.apgeochem.2006.04.006

Frondini, F., Caliro, S., Cardellini, C., Chiodini, G., Morgantini, N., Parello, F., 2008. Carbon dioxide degassing from Tuscany and Northern Latium (Italy). Glob. Planet. Change 61, 89–102. doi:10.1016/j.gloplacha.2007.08.009

Garofalo, K., Tassi, F., Vaselli, O., Delgado-Huertas, a., Tedesco, D., Frische, M., Hansteen, T.H., Poreda, R.J., Strauch, W., 2007. Fumarolic gases at Mombacho volcano (Nicaragua): Presence of magmatic gas species and implications for volcanic surveillance. Bull. Volcanol. 69, 785–795. doi:10.1007/s00445-006-0108-z

Gerlach, T., Graeber, E., 1985. Volatile budget of Kilauea volcano. Nature 313, 273–277.

Gerlach, T.., Doukas, M.., McGee, K.., Kessler, R., 2001. Soil efflux and total emission rates of magmatic CO2 at the Horseshoe Lake tree kill, Mammoth Mountain, California, 1995–1999. Chem. Geol. 177, 101–116. doi:10.1016/S0009-2541(00)00385-5

Gherardi, F., Panichi, C., Yock, A., Gerardo-Abaya, J., 2002. Geochemistry of the surface and deep fluids of the Miravalles volcano geothermal system (Costa Rica), Geothermics. doi:10.1016/S0375-6505(01)00030-X

Giggenbach, F., 1975. A simple method for the collection and analysis of volcanic gas samples. Bull. Volcanol. 39, 132–145.

Giggenbach, W.F., 1995. Variations in the Chemical and Isotopic Composition of Fluids Discharged from the Taupo Volcanic Zone, New-Zealand. J. Volcanol. Geotherm. Res. 68, 89–116. doi:10.1016/0377-0273(95)00009-J

Giggenbach, W.F., 1987. Redox processes governing the chemistry of fumarolic gas discharges from White Island, New Zealand. Appl. Geochemistry 2, 143–161. doi:10.1016/0883-2927(87)90030-8

Giggenbach, W.F., Soto, R.C., 1992. Isotopic and chemical composition of water and steam discharges from volcanic-magmatic-hydrothermal systems of the Guanacaste Geothermal Province, Costa Rica. Appl. Geochemistry 7, 309–332. doi:10.1016/0883-2927(92)90022-U

Gillot, P.-Y., Chiesa, S., Alvarado, G., 1994. Chronostratigraphy of upper miocene-quaternary volcanism in northern Costa Rica. Rev. Geol. Amér. Cent. 1, 45–53.

Hernández, P.A., Pérez, N.M., Salazar, J.M., Nakai, S., Notsu, K., Wakita, H., 1998. Diffuse emission of carbon dioxide, methane, and helium-3 from Teide Volcano, Tenerife, Canary Islands. Geophys. Res. Lett. 25, 3311–3314. doi:10.1029/98GL02561

Hinkle, M.E., 1994. Environmental conditions affecting concentrations of He, CO2, O2 and N2 in soil gases. Appl. Geochemistry 9, 53–63. doi:10.1016/0883-2927(94)90052-3

Hoefs, J., 1987. Stable Isotope Geochemistry, Springer Verlag.

Keeling, C.D., 1961. The concentration and isotopic abundances of carbon dioxide in rural and marine air. Geochim. Cosmochim. Acta 24, 277–298. doi:10.1016/0016-7037(61)90023-0

Kellogg, J.N., Vega, V., 1995. Tectonic development of Panama, Costa Rica, and the Colombian Andes: Constraints from global positioning system geodetic studies and gravity. Geol. Tecton. Dev. Caribb. Plate Bound. South. Cent. Am. 295, 75–90. doi:10.1130/SPE295-p75

Kempter, K. a., Benner, S.G., Williams, S.N., 1996. Rincón de la Vieja volcano, Guanacaste province, Costa Rica: geology of the southwestern flank and hazards implications. J. Volcanol. Geotherm. Res. 71, 109–127. doi:10.1016/0377-0273(95)00072-0

Kempter, K. a., Rowe, G.L., 2000. Leakage of active crater lake brine through the north flank at Rincon de la Vieja volcano, northwest Costa Rica, and implications for crater collapse. J. Volcanol. Geotherm. Res. 97, 143–159. doi:10.1016/S0377-0273(99)00181-X

Kitchen, C., 2002. La estratigrafía de depósitos volcanes y la actividad termal asociada con el complejo volcán Tenorio.

Kitchen, C.H., 2003. Petrologic and Geochemical Analysis of Volcanic Deposits in the Tenorio Volcanic Complex , Bijagua , Northwestern Costa Rica. Colorado College.

Lewicki, J.L., Bergfeld, D., Cardellini, C., Chiodini, G., Granieri, D., Varley, N., Werner, C., 2005. Comparative soil CO2 flux measurements and geostatistical estimation methods on Masaya volcano, Nicaragua. Bull. Volcanol. 68, 76–90. doi:10.1007/s00445-005-0423-9

Lewicki, J.L., Birkholzer, J., Tsang, C.F., 2007. Natural and industrial analogues for leakage of CO2 from storage reservoirs: Identification of features, events, and processes and lessons learned. Environ. Geol. 52, 457–467. doi:10.1007/s00254-006-0479-7

Marini, L., Yock Fung, A., Sanchez, E., 2003. Use of reaction path modeling to identify the processes governing the generation of neutral Na-Cl and acidic Na-Cl-SO4 deep geothermal liquids at Miravalles geothermal system, Costa Rica. J. Volcanol. Geotherm. Res. 128, 363–387. doi:10.1016/S0377-0273(03)00226-9

Melián, G., Hernández, P. a, Padrón, E., Pérez, N.M., Barrancos, J., Padilla, G., Dionis, S., Rodríguez, F., Calvo, D., Nolasco, D., 2014. Spatial and temporal variations of diffuse CO2 degassing at El Hierro volcanic system: Relation to the 2011-2012 submarine eruption. J. Geophys. Res. 119, 6976–6991. doi:10.1002/2014JB011013.Received

Melián, G. V, Pérez, N.M., Hernández, P. a, Salazar, J.M.L., Yock, A., Sánchez, E., Alvarado, G.E., Sumino, H., Notsu, K., 2004. Emisión Difusa de Dióxido de Carbono y Vaport de Mercurio en el Volcán Miravalles, Costa Rica. Rev. Geológica Am. Cent. 30, 179–188.

Molina, F., Marti, J., Aguirre, G., Vega, E., Chavarria, L., 2014. Stratigraphy and structure of the Canas Dulces caldera (Costa Rica). Geol. Soc. Am. Bull. 126, 1465–1480. doi:10.1130/B31012.1

Montegrossi, G., Tassi, F., Vaselli, O., Buccianti, a., Garofalo, K., 2001. Sulfur species in volcanic gases. Anal. Chem. 73, 3709–3715. doi:10.1021/ac001429b

Moya, P., Yock, A., 2005. First Eleven Years of Exploitation At the Miravalles Geothermal Field, in: Thirtieth Workshop on Geothermal Reservoir Engineering. p. 8.

Notsu, K., Mori, T., Do Vale, S.C., Kagi, H., Ito, T., 2006. Monitoring quiescent volcanoes by diffuse CO2 degassing: Case study of Mt. Fuji, Japan. Pure Appl. Geophys. 163, 825–835. doi:10.1007/s00024-006-0051-0

Padrón, E., Hernández, P. a., Toulkeridis, T., Pérez, N.M., Marrero, R., Melián, G., Virgili, G., Notsu, K., 2008. Diffuse CO2 emission rate from Pululahua and the lake-filled Cuicocha calderas, Ecuador. J. Volcanol. Geotherm. Res. 176, 163–169. doi:10.1016/j.jvolgeores.2007.11.023

Sigurdsson, H., Houghton, B., Rymer, H., Stix, J., McNutt, S., 1999. Encyclopedia of Volcanoes. Academic Press.

Smithsonian, 2015a. Miravalles [WWW Document].
URL: http://www.volcano.si.edu/volcano.cfm?vn=345030

Smithsonian, 2015b. Rincón de la Vieja [WWW Document].
URL: http://www.volcano.si.edu/volcano.cfm?vn=345020

Smithsonian, 2015c. Tenorio [WWW Document].
URL: http://www.volcano.si.edu/volcano.cfm?vn=345031

Soto, G. J., Alvarado, G. E., Goold, S., 2003. Erupciones <3800 a.P. del Volcán Rincón de la Vieja, Costa Rica. Rev. Geológica Amßerica Cent. 29, 67–86.

Tassi, F., Vaselli, O., Capaccioni, B., Giolito, C., Duarte, E., Fernandez, E., Minissale, a., Magro, G., 2005. The hydrothermal-volcanic system of Rincon de la Vieja volcano (Costa Rica): A combined (inorganic and organic) geochemical approach to understanding the origin of the fluid discharges and its possible application to volcanic surveillance. J. Volcanol. Geotherm. Res. 148, 315–333. doi:10.1016/j.jvolgeores.2005.05.001

Vaselli, O., Giordano, T., Capaccioni, B., Giannini, L., 2006. Sampling and analysis of volcanic gases 18, 65–76.

Vaselli, O., Tassi, F., Duarte, E., Fernandez, E., Poreda, R.J., Delago Huertas, A., 2010. Evolution of fluid geochemistry at the Turrialba volcano (Costa Rica) from 1998 to 2008. Bull. Volcanol. 72, 397–410. doi:10.1007/s00445-009-0332-4

Vaselli, O., Tassi, F., Giolito, C., Martínez, E., Fernández, E., Duarte, E., Barquero, J., Capaccioni, B., Van Bergen, M.J., 2003. Geochemistry and fluid circulation at the Tenorio volcanic complex (Costa Rica), in: Geoitalia.

Verbovsek, T., 2011. A comparison of parameters below the limit of detection in geochemical analyses by substitution methods. RMZ - Mater. Geoenvirontment 58, 393–404.

Werner, C., Cardellini, C., 2006. Comparison of carbon dioxide emissions with fluid upflow, chemistry, and geologic structures at the Rotorua geothermal system, New Zealand. Geothermics 35, 221–238. doi:10.1016/j.geothermics.2006.02.006

Werner, C., Hurwitz, S., Evans, W.C., Lowenstern, J.B., Bergfeld, D., Heasler, H., Jaworowski, C., Hunt, a., 2008. Volatile emissions and gas geochemistry of Hot Spring Basin, Yellowstone National Park, USA. J. Volcanol. Geotherm. Res. 178, 751–762. doi:10.1016/j.jvolgeores.2008.09.016

Williams, S.N., Lowe, D.R., Stoiber, R.E., Gemmell, J.B., Connor, C.B., Garcia, N., Londono, A., 1986. Eruption of the Nevado del Ruiz Volcano, Colombia, on 12 November 1985: Gas Flux and Fluid Geochemistry. Science (80-.). 233, 964–967.